OPEN ACCESS Freely available online

PLoS COMPUTATIONAL BIOLOGY

The Rates of Protein Synthesis and Degradation Account for the Differential Response of Neurons to Spaced and Massed Training Protocols

Faisal Naqib[1], Carole A. Farah[2], Christopher C. Pack[1,2], Wayne S. Sossin[2]*

1 Department of Physiology, Montreal Neurological Institute, McGill University, Montreal, Quebec, Canada, **2** Department of Neurology and Neurosurgery, Montreal Neurological Institute, McGill University, Montreal, Quebec, Canada

Abstract

The sensory-motor neuron synapse of *Aplysia* is an excellent model system for investigating the biochemical changes underlying memory formation. In this system, training that is separated by rest periods (spaced training) leads to persistent changes in synaptic strength that depend on biochemical pathways that are different from those that occur when the training lacks rest periods (massed training). Recently, we have shown that in isolated sensory neurons, applications of serotonin, the neurotransmitter implicated in inducing these synaptic changes during memory formation, lead to desensitization of the PKC Apl II response, in a manner that depends on the method of application (spaced versus massed). Here, we develop a mathematical model of this response in order to gain insight into how neurons sense these different training protocols. The model was developed incrementally, and each component was experimentally validated, leading to two novel findings: First, the increased desensitization due to PKA-mediated heterologous desensitization is coupled to a faster recovery than the homologous desensitization that occurs in the absence of PKA activity. Second, the model suggests that increased spacing leads to greater desensitization due to the short half-life of a hypothetical protein, whose production prevents homologous desensitization. Thus, we predict that the effects of differential spacing are largely driven by the rates of production and degradation of proteins. This prediction suggests a powerful mechanism by which information about time is incorporated into neuronal processing.

Citation: Naqib F, Farah CA, Pack CC, Sossin WS (2011) The Rates of Protein Synthesis and Degradation Account for the Differential Response of Neurons to Spaced and Massed Training Protocols. PLoS Comput Biol 7(12): e1002324. doi:10.1371/journal.pcbi.1002324

Editor: Jason M. Haugh, North Carolina State University, United States of America

Received May 30, 2011; **Accepted** November 10, 2011; **Published** December 29, 2011

Funding: F.N. was supported by an Alexander Graham Bell Canada Graduate Scholarship from the National Sciences and Engineering Research Council. C.A.F. is a postdoctoral fellow of the Fonds de la Recherche en Santé du Quebec (FRSQ) and a Conrad Harrington fellow. C.C.P. holds a Tier II Canada Research Chair. W.S.S. is a James McGill Professor and an FRSQ Chercheur National. This work was supported by a Canadian Institutes of Health Research (CIHR) grant MOP12046 to W.S.S., and a Canadian Excellence in Commercialization and Research (CECR) grant to the Montreal Neurological Institute. The funders had no role in study design, data collection and analysis, decision to publish, or preparation of the manuscript.

Competing Interests: The authors have declared that no competing interests exist.

* E-mail: wayne.sossin@mcgill.ca

Introduction

Different patterns of training can lead to different types and strengths of memories. For example, training distributed over time (spaced training) is superior to the equivalent amount of training with no interruptions (massed training) for generating long-term memories for verbal tasks [1]. Spaced and massed training are known to activate different molecular signaling pathways underlying memory formation [2]. *Aplysia californica*, a marine mollusk, provides an ideal model system for examining the differences in molecular signaling mediated by spaced and massed training [3].

One form of behavioral sensitization in *Aplysia* involves an increase in defensive reflexes after a noxious stimulus. The increase in defensive reflexes is caused in part by an increase, or facilitation, of the strength of the synapse between the mechanoreceptor sensory neurons and withdrawal motor neurons [4]. Facilitation is mediated by release of serotonin (5HT) from interneurons activated by the noxious stimulus [5,6]. Spaced noxious stimuli are superior to massed stimuli at generating long-term sensitization in the animal [3] and spaced applications of 5HT are superior to massed applications at generating long-term facilitation (LTF) of cultured sensory-motor neuron synapses [7]. The ability to examine the difference between spaced and massed training in cultured neurons allows the study of the differential signaling events activated by spaced and massed training.

5HT acts through at least two distinct G protein coupled receptors (GPCRs) in *Aplysia* to activate protein kinase A and protein kinase C [8,9]. The two kinases are differentially activated based on the type of training; spaced applications of 5HT lead to the persistent activation of PKA in the sensory neuron [10,11], while massed applications of 5HT instead activate both PKA and the novel PKC Apl II in the sensory neuron (Figure 1) [10,12].

An important mechanism for the differential activation of PKC during spaced and massed applications of 5HT involves differential desensitization of PKC Apl II translocation to the plasma membrane, where it is activated [13]. Spaced training (5×5 min 5HT with 15 min wash periods in between) leads to more desensitization than one massed 25 min application of 5HT [13]. This differential desensitization is surprising, since spaced applications of 5HT allow the neuron to recover in between exposures; yet they cause a greatly increased amount of desensitization when compared to the massed application of 5HT. This effect was shown to depend on both PKA-mediated desensitization and the downstream effects of protein synthesis

Author Summary

Memories are among an individual's most cherished possessions. One factor that has been shown to exert a powerful influence on memory formation is the pattern of training. Learning trials distributed over time have been shown to consistently produce longer lasting memories than trials distributed over short intervals, in every organism in which this has been studied. This observation has been investigated particularly well in the marine mollusk *Aplysia californica*. The nervous system of *Aplysia* is simple and well characterized, yet capable of forming memories, making it an ideal system for the study of learning and memory. Currently, we have a detailed understanding of memory formation in *Aplysia* at the cellular level. However, there remain many unanswered questions at the molecular level, particularly concerning how the effects of different patterns of learning are mediated. We have developed a mathematical model of a molecular signaling pathway known to underlie memory formation in *Aplysia*. Our model suggests that the rates of synthesis and degradation of proteins involved in memory regulation are essential for neurons of *Aplysia* to respond differentially to spaced and massed training. We were able to experimentally validate these findings, thus providing significant evidence for this model, which might underlie memory formation in more complex animals.

[13]. Importantly, protein synthesis inhibitors have opposite effects depending on the training stimulus: massed training produces a protein that prevents desensitization of PKC Apl II translocation while spaced training produces a protein that promotes desensitization of PKC Apl II translocation (Figure 1) [13]. Thus, another important distinction between these two training paradigms is that they activate distinct translational pathways.

While massed applications of 5HT are less effective than spaced applications at generating LTF measured at 24 h [7], both spaced and massed training lead to protein-synthesis dependent intermediate-term facilitation (ITF), measured 30 min to 2 hr after 5HT is removed [11,14,15]. However, the mechanisms underlying ITF induced by spaced or massed training are distinct; ITF induced by spaced training require PKA but not PKC for induction [16,17], while ITF induced by massed training, even a continuous stimulus as short as 10 min, requires PKC but not PKA [14] (Figure 1). Thus, the differential activation of PKC during massed and spaced training appears critical for the different physiological effects of these two training paradigms.

In order to better understand the signaling pathway mediating the desensitization of PKC Apl II, we developed a model consisting of a system of integro-differential equations describing the differential desensitization of PKC Apl II activation during massed and spaced training. The model provides predictions about the molecular mechanisms responsible for the differences between massed and spaced training. These predictions were validated with new experiments. Together these results suggest that the sensitivity of neurons to the time between training periods is due to the rates of protein synthesis and degradation.

Results

Describing the model architecture

We have previously described PKC Apl II translocation and its desensitization in response to 5HT application in the presence of PKA and protein synthesis inhibitors [13,18,19]. We showed that PKC translocation differentially desensitizes to spaced and massed applications of 5HT, and that this differential desensitization was dependent on protein translation and PKA activity. In order to understand the molecular mechanisms underlying desensitization of PKC Apl II translocation we designed a signaling network

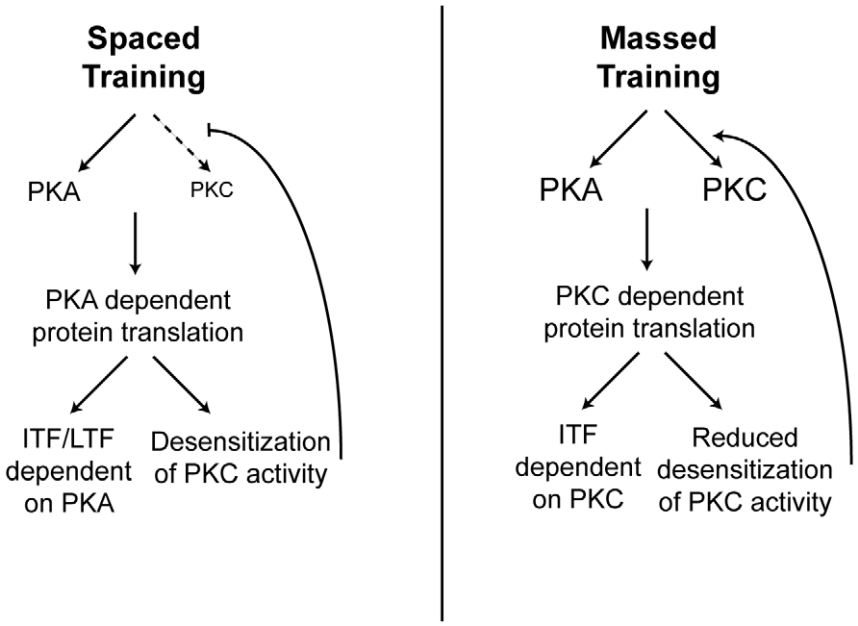

Figure 1. Massed versus spaced application of 5HT. Spaced training activates PKA but not PKC and leads to PKA-dependent translation that induces intermediate-term facilitation (ITF) and long-term facilitation (LTF) not dependent on PKC. PKA dependent translation also produces a protein that increases PKC desensitization, which is required for spaced training not to activate PKC. Massed training activates both PKA and PKC and leads to PKC-dependent translation that induces a distinct form of ITF not dependent on PKA. PKC-dependent translation also produces a protein that prevents PKC desensitization, which is required for massed training to continually activate PKC.
doi:10.1371/journal.pcbi.1002324.g001

based on our previous experimental findings and biochemical mechanisms known to underlie G protein-coupled receptor (GPCR) desensitization. Our network consists of the translocation of PKC, the cycling of a GPCR, the translation of two hypothetical proteins, and activity of PKA. We have tried to simplify the network whenever possible, including bundling multiple biochemical reactions into one single rate in order to simplify its architecture. The reasoning behind the network's architecture is given in this section and the model equations are given in the Materials and Methods section.

The basic unit of the model is the 5HT GPCR (S) that once activated leads to the production of diacylglycerol (DAG), which is capable of activating and translocating PKC Apl II to the membrane [20,21]. While this pathway consists of multiple steps, such as G-protein activation of phospholipase C and phospholipase D [18], these are not likely to be important for modeling of desensitization, since in most systems the amount of the activatable GPCR is the rate-limiting quantity that is decreased during desensitization [22,23,24].

GPCRs can enter a number of different pathways, such that S can exist in several different states, where the change in concentration of each state with respect to time is modeled. The base component of our model includes the activation and inactivation of S without any desensitization dynamics. This component corresponds to how quickly PKC Apl II translocates to the membrane after 5HT application and how quickly it dissociates from the membrane after 5HT is washed away. It is known that application of 5HT results in a maximal translocation of PKC Apl II within one minute, after which it remains at this maximal level for at least five minutes [18,19]. Washing off 5HT prompts the complete dissociation of PKC Apl II within one minute [13,18,25]. To replicate these findings, we used a simple network architecture, whereby in the presence of 5HT, S_{OFF} becomes S_{ON}, which then transforms to S_{IN1}. S_{OFF} represents the inactivated receptor that can become activated by 5HT, turning S_{OFF} into S_{ON}, which then produces DAG allowing for the translocation of PKC Apl II. S_{IN1} is an inactivated receptor that needs to be recycled before it can become activated by 5HT again. At a biochemical level, the transitions from S_{ON} to S_{IN1} to S_{OFF} involve multiple molecular steps including GPCR phosphorylation by G protein receptor kinases, binding of beta arrestin, possible internalization of the receptor, unbinding of the ligand, and then recycling of the receptor back to its initial state [22,23,24]. For simplicity, we have reduced these multiple steps into the two steps (S_{ON} to S_{IN1} to S_{OFF}) since (i) this is sufficient to capture the behavior required to understand the questions we are addressing (see below) and (ii) we have no specific knowledge concerning regulation of these pathways in *Aplysia*. The major constraint from the data is that PKC comes off the membrane in less than one minute after 5HT is washed off. Thus S_{ON} to S_{IN1} must be fast enough to account for this inactivation. However, in the first 5 min of 5HT activation, there is little desensitization of PKC Apl II translocation. Thus, S_{IN1} to S_{OFF} must be rapid enough to prevent appreciable desensitization in the first five minutes. The transitions between states of S were modeled using mass action kinetics. These model parameters were fit to the previously described PKC dynamics [13,18,25] (equations, parameter values, and parameter estimation methods can be found in the Materials and Methods section). Once an appropriate fit was found these parameters were set and we were able to begin expanding the model and modeling data related to PKC Apl II desensitization.

The complete model architecture is presented in Figure 2. The model components (color coded) were developed sequentially, with maroon and black first then blue, red, and finally green. The

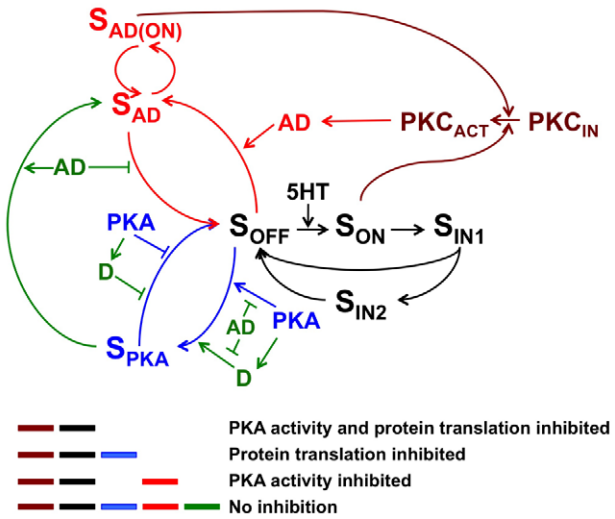

Figure 2. Complete model network. The maroon network describes the translocation of PKC to the plasma membrane and its subsequent dissociation from the membrane. The module denoted in black represents the homologous desensitization pathway. The blue network defines the PKA mediated desensitization of PKC Apl II. The red network illustrates the AD pathway responsible for the rescuing PKC from desensitization. Finally the D pathway, which is antagonistic to the AD pathway and causes the increase in desensitization, is specified by the green network. In green are the additional roles of AD needed to counteract D during massed training.
doi:10.1371/journal.pcbi.1002324.g002

maroon component represents only the translocation of PKC to the plasma membrane and its subsequent dissociation from the membrane. The black component represents the desensitization pathway in the presence of a protein translation inhibitor and a PKA inhibitor. In the presence of these inhibitors, PKC Apl II translocation desensitizes during exposure to 5HT [13]. Thus, there must be a protein translation-independent and PKA-independent desensitization pathway, or a homologous desensitization pathway, which we model as an alternate recycling pathway from S_{IN1} to S_{OFF}, passing through S_{IN2} (Figure 2; black network only, equations can be found in the Materials and Methods section). Here S_{IN2} acts as a secondary inactivated state that requires a longer processing time than S_{IN1} before recycling back to S_{OFF}. At the biochemical level, this represents the sorting of the GPCR in the endocytic compartment from a rapid recycling pathway into a slow recycling pathway or degradative pathway. This architecture was chosen because of the abundant literature supporting this mechanism for desensitization of GPCRs [22,23,24].

PKA, which is activated by 5HT, has been shown to increase desensitization of PKC Apl II translocation in the absence of protein translation [13]. The condition where PKA is active and protein translation is inhibited is modeled by the combination of the black, maroon, and blue components. In order to model PKA-mediated protein synthesis-independent desensitization, we included a reduced and modified version of a previous model of PKA activity [26]. Our modifications to this PKA model are described in the next sections. Activity of PKA is capable of converting S_{OFF} directly into S_{PKA}, where S_{ON} is not immediately attainable and PKC Apl II cannot be activated (Figure 2; black and blue networks, equations can be found in the Materials and Methods section). At the biochemical level, this network would represent phosphorylation of the receptor, or receptor-associated protein, by PKA causing the endocytosis of the GPCR from the

plasma membrane to an endocytic compartment distinct from S_{IN1} and S_{IN2}, probably representing a regulated recycling endosome [27]. It is important to note that since PKA can convert S_{OFF} to S_{PKA}, conversion to S_{PKA} does not require S to go through the active state, S_{ON}, such as the desensitization mediated by S_{IN2}. This network architecture is required to account for the observation that PKA activity between pulses of 5HT, when S would not be activated, is capable of desensitizing PKC Apl II translocation [13] and is consistent with data on heterologous desensitization of GPCRs in other systems [28]. This consideration also removed the alternate topology where S_{PKA} would represent alternate sorting from S_{IN1}, since the receptor is only in the S_{IN1} state when the receptor goes through the active state.

The recycling of S_{PKA} back into S_{OFF} is inhibited by PKA. This inhibition was not initially part of the architecture, but it was not possible to replicate both the massed training and spaced training data sets without including the PKA inhibition of S_{PKA} recycling (see results below). At a biochemical level, this suggests that PKA activity is not only required to induce sorting of the receptor to the regulated recycling endosome but its retention in this compartment as well.

The reverse situation, with PKA activity inhibited but protein translation allowed to function is modeled by the combination of the black, maroon, and red components. Protein translation in the absence of PKA activity leads to a reduction in the desensitization of PKC Apl II translocation only during massed 5HT application and not spaced [13]. This observation requires that a protein, which protects PKC Apl II translocation from the constitutive desensitization pathway be translated during massed training. We name this hypothetical protein Anti-Desensitizer (AD) and its effects on the network are represented by the black, maroon and red components combined. We modeled the mechanism of AD mediating this protection by having AD convert S_{OFF} into S_{AD}, a form of S preserved from the desensitization pathways leading to S_{IN2} or S_{PKA}, but similar to S_{OFF} in its ability to become activated by 5HT and cause the translocation of PKC Apl II (Figure 2, black, maroon and red pathway; equations can be found in the Materials and Methods section). At the biochemical level, this would represent the AD protein binding to the receptor, or receptor associated protein, preventing its inactivation and internalization [29,30,31,32]. Since a protein-synthesis dependent protection from desensitization is seen in massed, but not spaced, training protocols, we would expect AD to be synthesized only after massed training. In order for this differential synthesis to occur, we made production of AD proportional to the mathematical integration of the level of active PKC Apl II. PKC Apl II is constantly active during massed training, but not during spaced training; thus, integrating PKC activity allows for selective activation of AD during massed training. PKC is known to regulate the translational machinery in many systems [33,34] including *Aplysia* [35,36], but the exact mechanism by which PKC regulates translation in this case is not known and is not explicitly modeled here.

Finally, allowing both protein translation and PKA activity to proceed normally results in an increase in the desensitization of PKC Apl II translocation during spaced training [13]. This increase in desensitization was observable only when both PKA activity and protein translation are allowed to proceed, meaning a translated protein is mediating this increase in desensitization, and its rate of translation is dependent on PKA activity. We name this hypothetical protein Desensitizer (D), and we model its mechanism of action similarly to that of PKA by transforming S_{OFF} into S_{PKA} and inhibiting its recycling back to S_{OFF} (Figure 2, complete network; equations can be found in the Materials and Methods section). Another possible architecture would have been to generate another state of S (S_D), but there was not a good biochemical rationale for this and the model worked well (see below) without this additional state. At the biochemical level, D would be a protein that promotes endocytosis [29], particularly to the PKA-dependent pathway. The rate of translation of D is dependent on the amount of PKA activity, similar to the dependence of AD translation on PKC Apl II activity. One difference between the translation of D and AD is that D's production is delayed by 10 min after its induction. The use of a delay was necessary to account for the observation that desensitization of PKC Apl II translocation after a 5 min pulse of 5HT did not begin until after a 10 min wash [13]. At a biochemical level, there may be many reasons for a delay, ranging from requirements for post-translational modification, cellular trafficking, or delay in the activation of proteins synthesis. Finally, while trying to model the data we found that for D to cause enough desensitization during spaced training resulted in too powerful an inhibition during massed training. This over-inhibition resulted from the fact that unlike AD, D is synthesized during both spaced and massed training since PKA is active in both scenarios [10]. To diminish the role of D during massed training, we introduced two additional effects of the AD protein. First, AD inhibited the transition from S_{OFF} to S_{PKA}, and second, it could transform not only S_{OFF} to S_{AD} but also S_{PKA} to S_{AD} (Figure 2; complete network). At a biochemical level, this corresponds to the ability of the AD protein to prevent endocytosis to the PKA-dependent pathway, and moreover, to bind to the GPCR in the regulated recycling endosome and enhance its recycling, similar to the mechanism by which decreased PKA activity enhanced recycling from this compartment. We also attempted to model the system with AD preventing the translation of D as opposed to opposing its actions, but were unable to achieve a good fit to the data with this architecture.

For simplicity, we made the assumption that during the time course of our experiments an insignificant amount of new S is created. This assumption was also made partially because for S to enter the S_{OFF} state, the GPCR would not only have to be synthesized, but processed through the endoplasmic reticulum, Golgi apparatus, and transported back to the membrane, so new S could only contribute to the later parts of the experimental paradigm. We do not have a term for destruction of S, however, as described below, the S_{IN2} pathway may be equivalent to a degradation pathway, where the GPCR enters late endosomes and lysosomes.

Modeling the homologous desensitization pathway finds slow rate of recovery from desensitization

PKC Apl II translocation still desensitizes during exposure to 5HT even when both protein translation and PKA have been inhibited [13]. Thus, there must be a homologous desensitization pathway (Figure 3A; black network only, equations can be found in the Materials and Methods section). Parameter values were estimated by fitting the model to PKC Apl II translocation measurements taken during a continuous 90 min application of 5HT in the presence of the protein translation inhibitor anisomycin and the PKA inhibitor KT5720 [13]. Several parameter estimation methods were used, and surprisingly, all of them yielded recycling rates of S_{IN2} back to S_{OFF} (k_{A5}) that were near zero (parameter values can be found in Table 1), resulting in an excellent fit to the data as can be seen in Figure 3C ($R^2>0.99$). Note that throughout the paper, data presented in blue represents data obtained from Farah et al. (2009) used to train the model, while data presented in red represents experiments performed to

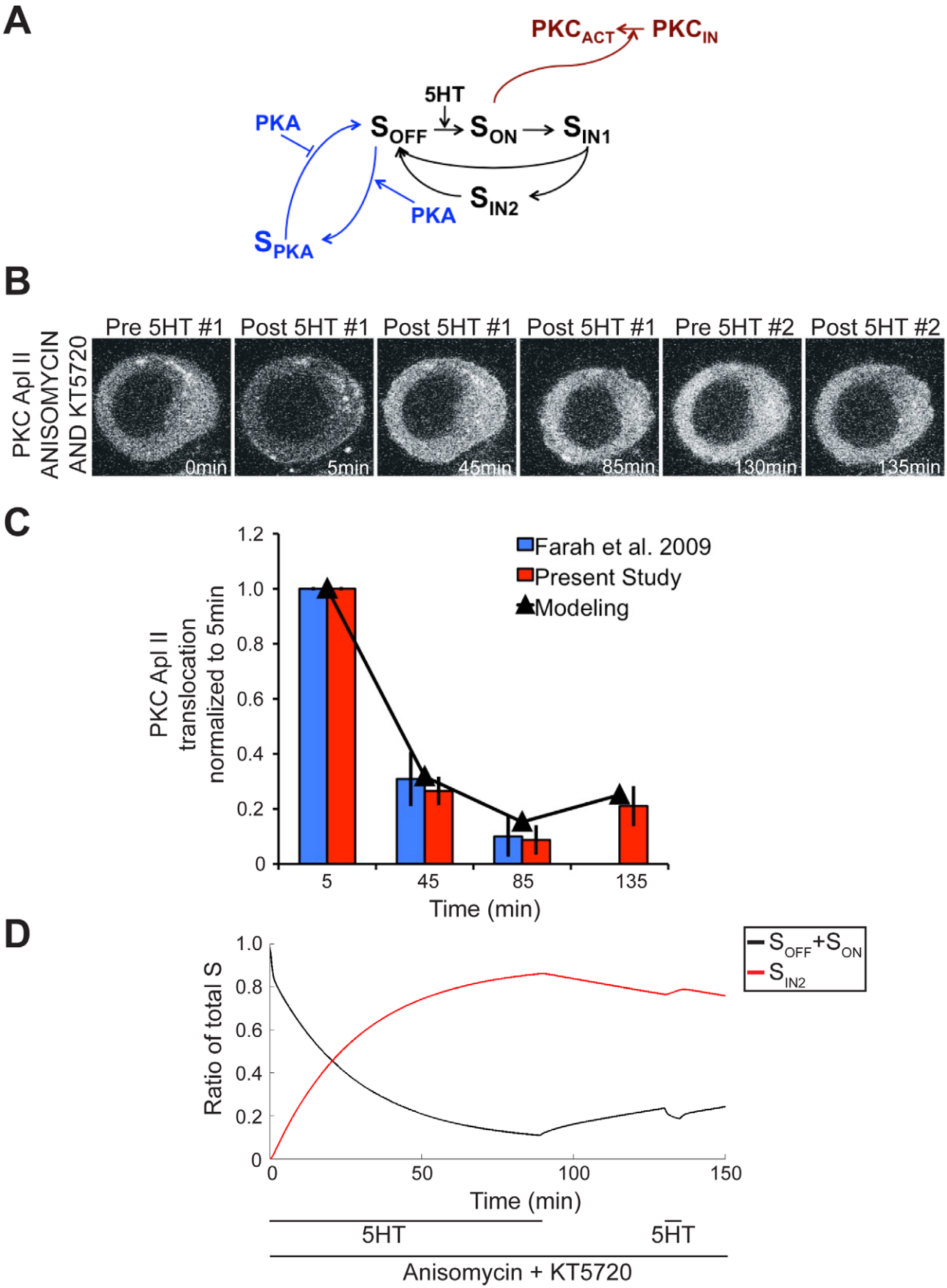
A
PKC_ACT
PKC_IN
5HT
PKA
S_OFF
S_ON
S_IN1
S_IN2
PKA
S_PKA
B
PKC Apl II
ANISOMYCIN
AND KT5720
Pre 5HT #1
Post 5HT #1
Post 5HT #1
Post 5HT #1
Pre 5HT #2
Post 5HT #2
0min
5min
45min
85min
130min
135min
C
PKC Apl II
translocation
normalized to 5min
Farah et al. 2009
Present Study
Modeling
1.2
1.0
0.8
0.6
0.4
0.2
0
5
45
85
135
Time (min)
D
Ratio of total S
S_OFF+S_ON
S_IN2
1.0
0.8
0.6
0.4
0.2
0
0
50
100
150
Time (min)
5HT
5HT
Anisomycin + KT5720

Figure 3. Modeling and experimental validation of homologous desensitization pathway. A, Model network pathways of homologous desensitization pathway (black) and PKA-mediated desensitization pathway (black and blue). **B**, Representative confocal fluorescence images of sensory neurons expressing eGFP-PKC Apl II during a 90 min exposure to 5HT followed by a 45 min wash and then a 5 min 5HT application, all in the presence of anisomycin and KT5720. **C**, Quantification of PKC Apl II translocation (bars) and modeling output (line). Blue bars are data used from Farah et al. (2009) to fit the model parameters. Red bars are data from the present study (n = 8 cells). Error bars are SEM. **D**, Modeling of S dynamics in response to experimental protocol from **B**. Black line represents the ratio of S_{OFF} and S_{ON} to total S and the red line the ratio of S_{IN2} to total S. The times of addition of 5HT and pharmacological agents are indicated below the figure.
doi:10.1371/journal.pcbi.1002324.g003

confirm predictions of the model. The model predicted very little recycling of the signaling complex from S_{IN2} during massed training in the absence of protein translation and PKA activity (Figure 3C, D). This was unexpected, since our earlier experiments showed that the desensitization seen after a 5 min pulse of 5HT recovered completely within 45 min, suggesting efficient recycling of the signaling complex [13]. However, these experiments were not done in the presence of a PKA inhibitor.

To test the prediction of the model that desensitization seen in the absence of PKA activity was not reversible, we conducted a new experiment. The rate of S_{IN2} recycling was predicted to be slow enough that a wash period after massed training with anisomycin and KT5720 would result in little recovery of translocation to initial values. Thus, in a simulation of a 90 min exposure to 5HT followed by a 45 min wash and then a 5 min pulse of 5HT, all in the presence of anisomycin and KT5720, the 5 min pulse of 5HT should only cause a small amount of PKC Apl II translocation, since a majority of S is held in the inactivated state S_{IN2} (Figure 3C, D). To test this prediction of the model, we used this protocol in a new imaging experiment using *Aplysia* sensory neurons expressing eGFP-PKC Apl II. The initial massed training caused a similar amount of translocation to that previously observed by Farah et al. (2009) (Figure 3B, C). Furthermore, the amount of desensitization after the 5 min pulse of 5HT matched the modeling prediction extremely well, demonstrating that recovery from desensitization under these conditions was indeed very slow (Figure 3B, C).

This protocol required that the neurons be imaged for a total of 140 min. To ensure that the lengthy exposure to room temperature (20–23°C) and the drugs anisomycin and KT5720 had no effect on the health of the neurons, or their ability to translocate PKC Apl II, two 5 min pulses of 5HT were applied with a 130 min wash in between, all in the presence of both drugs. Recovery from a 5 min pulse of 5HT occurs after 45 min [13], so we expect that a 130 min wash should result in complete recovery and that any depression in PKC Apl II translocation would be caused by injury to the neurons due to prolonged exposure to room temperature and drugs. There was no significant difference in the amount of PKC Apl II translocation between the first and second pulse of 5HT (mean+/−sem; 1.08+/−0.18, n = 5). Thus the persistent desensitization observed in the previous experiment is due only to accumulation of S in S_{IN2}, as predicted by the model and not due to injury to the neurons.

Modeling desensitization induced by PKA confirms rapid rate of recovery

PKA, which is activated by 5HT, has been shown to increase desensitization of PKC Apl II translocation during both massed and spaced training [13]. In order to model PKA mediated desensitization, we included a reduced and modified version of a previous model of PKA activity [26]. We reduced the complexity of this model to only include only the dynamics of cAMP production and the association and dissociation of the subunits of PKA. This simplification was done since our experiments and simulations do not occur over long enough time periods for us to expect a contribution from the persistent activity of PKA, which was a major feature of their model. We modified the Pettigrew et al. model by altering the basal level of cAMP and the association rate of the PKA subunits to refine PKA dynamics to better match published data demonstrating PKA activity persisting for a small period after washout of 5HT [10,37,38]. This revision was necessary since PKA activity during the wash period is required for desensitization [13]. The new PKA dynamics to massed and spaced training can be seen in Figure 4A–C. Furthermore, we removed any synthesis or degradation of PKA subunits since, similar to PKC Apl II, we do not expect a significant change in the amount of protein during the time course of our experiments [10].

The black and blue networks (Figure 3A) make use of the previously described PKA activity model to affect the desensitization of PKC translocation. Two data sets were used to estimate the parameters of the blue component of the model: one continuous 90 min application of 5HT in the presence of anisomycin and five pulses of 5HT each lasting 5 min with 15 min washes in between, all in the presence of anisomycin [13]. The parameters were estimated to fit both data sets. The conversion of S_{OFF} into S_{PKA} is modeled using mass action kinetics. The recycling of S_{PKA} back into S_{OFF} is inhibited by PKA and is modeled using a combination of mass action kinetics and an inhibitory Hill function (see Materials and Methods section). This network architecture resulted in an excellent fit to both data sets ($R^2 = 0.99$ for massed training and 0.88 for spaced training) (Figures 4D, 5B). It was not possible to replicate both the massed training and spaced training data sets without including the PKA inhibition of S_{PKA} recycling. Without this inhibition, fitting the massed training data set caused too much desensitization during spaced training and fitting the spaced training data set caused insufficient desensitization during massed training.

Massed training in the absence of protein synthesis leads to more desensitization of PKC Apl II translocation when PKA is active [13]. However, the model predicts that soon after 5HT is washed away, PKA becomes inactive and S_{PKA} can recycle back to S_{OFF}. This recycling suggests that unlike S_{IN2} mediated desensitization, PKA induced desensitization recovers quickly. Thus, when we simulate a 90 min exposure to 5HT followed by a 45 min wash and then a 5 min pulse of 5HT (as above, but in the absence of a PKA inhibitor), the model predicts a considerable recovery of PKC translocation (Figure 5B, C). This recovery happens because during the 90 min stimulation, the majority of S is held in S_{PKA}, and during the wash most of S_{PKA} recycles back to S_{OFF}. This recycling allows for a greater amount of PKC translocation compared to when PKA was inhibited and the majority of S is found in S_{IN1} (Figure 3C). To test this prediction of the model, we conducted a new imaging experiment, measuring the translocation of eGFP-PKC Apl II during the application of the above protocol (Figure 5A). The translocation of PKC Apl II caused by the 5 min pulse of 5HT after the 45 min wash is in agreement with the modeling prediction, thus validating this component of the model (Figure 5B). The amount of desensitization of PKC Apl II translocation during the massed training is equivalent to that observed by Farah et al. (2009) and, as in that study, PKA increases the amount of desensitization during massed

Table 1. Model parameters.

Parameter	Value	Sensitivity (Spaced)	Sensitivity (Massed)	Notes (Found in Equation(s))
k_{A2}*	1	High	High	S_{ON} into S_{IN1} (2,4)
k_{S1a}	6	High	High	Half saturation of Hill function synthesizing AD (10)
k_{D3b}	0.3372	High	High	Hill coefficient of Hill function inhibiting S_{OFF} into S_{PKA} (via AD) (3,6)
k_{DAGp}*	200	High	High	DAG synthesis rate constant (1)
k_{DAGd}*	10^2	High	High	DAG degradation rate constant (1)
k_{A1}*	10^5	High	Medium	S_{OFF} into S_{ON} (2,3)
k_{S1b}	4	High	Medium	Hill coefficient of Hill function synthesizing AD (11)
k_{S3}	0.4483	High	Medium	D synthesis rate constant (13)
k_{A3}*	3	Medium	High	S_{IN1} to S_{OFF} (3,4)
k_{A4}*	0.2371	Medium	High	S_{IN1} to S_{IN2} (4,5)
k_{S3a}	6	Medium	High	Half saturation of Hill function synthesizing D (13)
delayD	10	Medium	High	PKA delay in D synthesis (14)
intPKA	15	Medium	High	PKA integration window (14)
k_{D3}	0.0764	Medium	Medium	S_{PKA} into S_{AD} (6,15)
k_{D3b}	0.1385	Medium	Medium	Hill coefficient of Hill function activating S_{PKA} into S_{AD} (6,15)
k_{S1}	0.026	Medium	Medium	AD synthesis rate constant (11)
k_{S2}	0.2	Medium	Medium	AD degradation rate constant (12)
k_{C1}	2	Medium	Medium	S_{OFF} into S_{AD} (3,15)
k_{C2}	0.1	Medium	Medium	S_{AD} into S_{OFF} (3,15)
k_{S4}	0.2847	Medium	Medium	D degradation rate constant (13)
k_{D1}	8.0441	Medium	Medium	S_{OFF} into S_{PKA} (via D) (3,6)
k_{D1a}	$5.33*10^{-8}$	Medium	Medium	Half saturation of Hill function inhibiting S_{OFF} into S_{PKA} (via AD) (3,6)
V_m	3.6	Medium	Medium	cAMP synthesis rate constant (7)
K_{fpka}	105	Medium	Medium	PKA subunit dissociation rate constant (8,9,10)
intPKC	15	Medium	Medium	PKC integration window (12)
k_{A5}	0.003	Low	Medium	S_{IN2} to S_{OFF} (3,5)
k_{B2a}	0.5	Low	Medium	Half saturation of Hill function inhibiting S_{PKA} into S_{OFF} (via PKA) (3,6)
k_{B2b}	6	Low	Medium	Hill coefficient of Hill function inhibiting S_{PKA} into S_{OFF} (via PKA) (3,6)
k_{C2b}	1	Low	Medium	Hill coefficient of Hill function inhibiting S_{AD} into S_{OFF} (3,15)
k_{B2}	0.2	Medium	Low	S_{PKA} into S_{OFF} (3,6)
k_{D2b}	0.4187	Medium	Low	Hill coefficient of Hill function inhibiting S_{PKA} into S_{OFF} (via D) (3,6)
K5HT	$14*10^{-6}$	Medium	Low	Half saturation of Hill function synthesizing cAMP (7)
K_{bpka}	3	Medium	Low	PKA subunit reassociation rate constant (8,9,10)
k_{B1}	0.1276	Low	Low	S_{OFF} into S_{PKA} (via PKA) (3,6)
k_{D3a}	$1.6*10^4$	Low	Low	Half saturation of Hill function transforming S_{PKA} into S_{AD} (6,15)
k_{C2a}	1	Low	Low	Half saturation of Hill function inhibiting S_{AD} into S_{OFF} (3,15)
k_{B2a}	53.1	Low	Low	Half saturation of Hill function inhibiting S_{PKA} into S_{OFF} (via D) (3,6)
$cAMP_{basal}$	0.005	Low	Low	Basal concentration of cAMP (7)
k_{S3b}	4	Low	Low	Hill coefficient of Hill function synthesizing D (13)

Parameter sensitivity analysis. Model parameters and their values. Sensitivity was determined by varying individual parameters by +/−5% and +/−50% while holding the other parameters at their defined values. The sensitivity of a parameter was classified as High if either a +/−5% change in its value caused a change in the fit of the data of over 25%. Similarly, the sensitivity of a parameter was Medium if either a +/−50% change in value caused a change in the fit of the data of over 25%, and Low if the +/−50% change in value did not change the fit by more than 25%. Two data sets were used to conduct this analysis: 90 min 5HT and 5×5 min 5HT with 15 min washes. List ordered by sensitivity to 5×5 min 5HT. Parameters indicted with a * were replaced with the following in an alternate model: $k_{A2}=2$, $k_{DAGp}=2$, $k_{DAGd}=200$, $k_{A1}=200{,}000$, $k_{A3}=2$, and $k_{A4}=0.08$.

doi:10.1371/journal.pcbi.1002324.t001

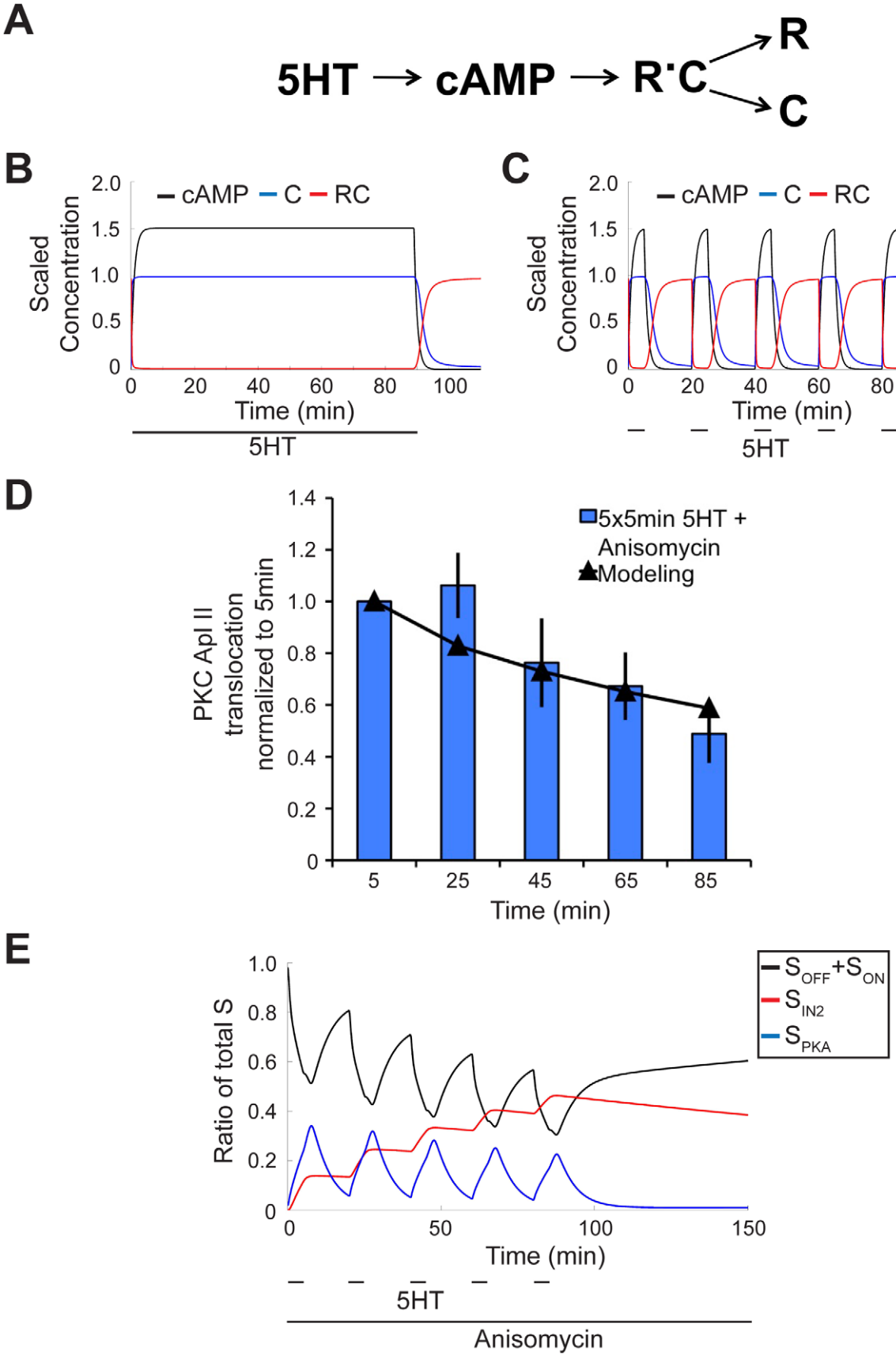

Figure 4. PKA dynamics. A, Model network pathway of PKA dynamics. R and C represent the regulatory subunit and catalytic subunit of PKA, respectively, where the amount of PKA activity is considered identical to C activity. **B**, **C**, PKA activity in response to a 90 min 5HT application (**B**) or 5×5 min 5HT application (**C**). Black line represents the amount of cAMP activity; blue line represents C, and red line RC. R is not shown, as it is

identical to C. (Model adapted from [70]). **D**, PKC Apl II translocation in response to 5×5 min application of 5HT with 15 min washes in between and anisomycin present throughout from Farah et al. (2009) (bars) and modeling output (line). **E**, Modeling of S dynamics in response to experimental protocol from **D**. Black line represents the ratio of S_{OFF} and S_{ON} to total S, the red line the ratio of S_{IN2} to total S, and the blue line represents ratio of S_{PKA} to total S.
doi:10.1371/journal.pcbi.1002324.g004

training. However, despite this increased desensitization in the presence of PKA, active PKA increases the recovery from desensitization, as predicted by the model. The large difference between the recovery in the presence or absence of the PKA inhibitor, KT5720, is illustrated in Figure 5D.

Rescue from desensitization by Anti-Desensitizer (AD) protein

The rescue from desensitization by the AD protein is modeled using the black and red network components in combination (Figure 6A, red pathway). Two data sets were used to estimate the parameters of this component of the model: 90 min application of 5HT in the presence of KT5720 and five 5 min pulses of 5HT with 15 min washes in between, all in the presence of KT5720 [13]. The model produced an excellent fit to both data sets ($R^2 = 0.95$ for spaced training and 0.99 for massed training) (Figure 6B, D). One of the unexpected predictions of the model was both a fast degradation of AD, (with a half-life of ~5 min) and a slow rate of the $S_{AD} \rightarrow S_{OFF}$ recycling.

To validate this component of the model, we designed a protocol that would be sensitive to the fast degradation rate of AD. This protocol consisted of exposure to 25 min of 5HT in the presence of KT5720 then 65 min of 5HT in the presence of both KT5720 and anisomycin, with no wash in between. This protocol allows for the indirect observation of the degradation of AD and the recycling of S_{AD} back into S_{OFF}. The addition of anisomycin will terminate the translation of AD. During these last 65 min, the model predicts that AD will decay and thus be less effective at transforming S_{OFF} into S_{AD} (Figure 6C). The model further predicts that the absence of AD will cause the remaining S_{AD} to recycle back into S_{OFF}, where it will lose its protection from the homologous desensitization pathway, which will manifest in decreased PKC Apl II translocation. Thus, by observing the increased amount of desensitization of this protocol in comparison to when AD translation is present throughout, we can validate the model's predicted rate of AD degradation and rate of S_{AD} recycling back into S_{OFF}. To test these predictions of the model, a new imaging experiment was performed by applying this protocol to *Aplysia* sensory neurons expressing eGFP-PKC Apl II. As expected, the amount of PKC translocation observed in these neurons during the first 25 min of 5HT was equivalent to that observed during the 25 min of massed training in the presence of KT5720, carried out by Farah et al. (2009) (Figure 6A, B). However, the final 65 min of this protocol, where both KT5720 and anisomycin are present, caused a lower amount of PKC Apl II translocation compared to that caused by massed training in the presence of only KT5720, in agreement with the model prediction ($R^2 = 0.99$) confirming the fast degradation rate of AD and the slow rate of S_{AD} to S_{OFF} (Figure 7C).

Modeling increase in desensitization by Desensitizer (D) protein

During spaced training, the desensitization of PKC Apl II translocation was increased in control cells in comparison to when protein translation was inhibited. This increase in desensitization was observable only when both PKA activity and protein translation are allowed to proceed, meaning a translated protein is mediating this increase and its rate of translation is dependent on PKA activity. We name this hypothetical protein Desensitizer (D), and its effects on PKC Apl II translocation are modeled by the green component of the network (Figure 2). Seven data sets were used to estimate the parameters of this component of the model: one continuous 90 min application of 5HT, five pulses of 5HT each lasting 5 min with 15 min washes in between, and five experiments, each with two pulses of 5HT each lasting 5 min but with a different wash period length (5 min, 10 min, 15 min, 30 min, 45 min,) in between the pulses [13] (Figure 8A, C, E). The resulting model formed an excellent fit to the data ($R^2 = 0.99$ for massed training, 0.99 for spaced training, and 0.75 for two pulses of 5HT with varying wash intervals). One exception is the 5 min pulse followed by a 5 min wash, where there is an increase in PKC Apl II translocation compared to the initial translocation, while our model shows no increase in translocation. We believe fitting this increase would require a more detailed dissection of the pathway between the GPCR and its downstream targets and is beyond the scope of this study.

Model successfully predicts the response to new spacing protocols

As one of the rationales for generating this model was to gain insight into the role of spacing, our final confirmation of the model tested an alternate spacing protocol. We designed an experiment that would require the functioning of all the model components and that made a specific prediction that was not obvious and could be tested. Interestingly, we found that if 15 min pulses of 5HT were used, the model predicted that longer washes would lead to increased desensitization. While 15 min pulses produce both D and AD, the model predicts that longer washes will reduce the levels of AD compared to D and thus predicts greater desensitization by longer washes (Figure 9B and E). In particular note that the model predicts that with the shorter spacing (Figure 9C), the amount of S complex in S_{AD} is larger than in S_{PKA} immediately before the second pulse, while with longer spacing (Figure 9F), the model predicts that there is more S complex in S_{PKA}, than in S_{AD}. Thus, the second pulse of serotonin during the protocol with longer spacing should be less able to translocate PKC Apl II because of the conversion of S_{AD} to S_{PKA}. To test this prediction, we performed a new imaging experiment where sensory neurons were exposed to three 15 min pulses of 5HT with either 15 min or 25 min washes in between the 5HT pulses. The results of this protocol are also sensitive to the delay and rate of D translation (parameters that had not yet been validated in a separate experiment). Both protocols were applied to *Aplysia* sensory neurons expressing eGFP-PKC Apl II. The amount of PKC translocation during both protocols matched the modeling prediction ($R^2 > 0.99$) (Figure 9A, B, D, and E) and thus validates this component of the model as well as the functioning of the completed model. In particular, to highlight the effect of the wash, we calculated the amount of desensitization during the 15 min or 25 min wash (e.g. the amount of translocation at the beginning of pulse 2 compared to the end of pulse 1, or the beginning of pulse 3 compared to the end of pulse 2). The model predicted more desensitization during the longer wash and this was confirmed by the imaging experiment (Figure 10).

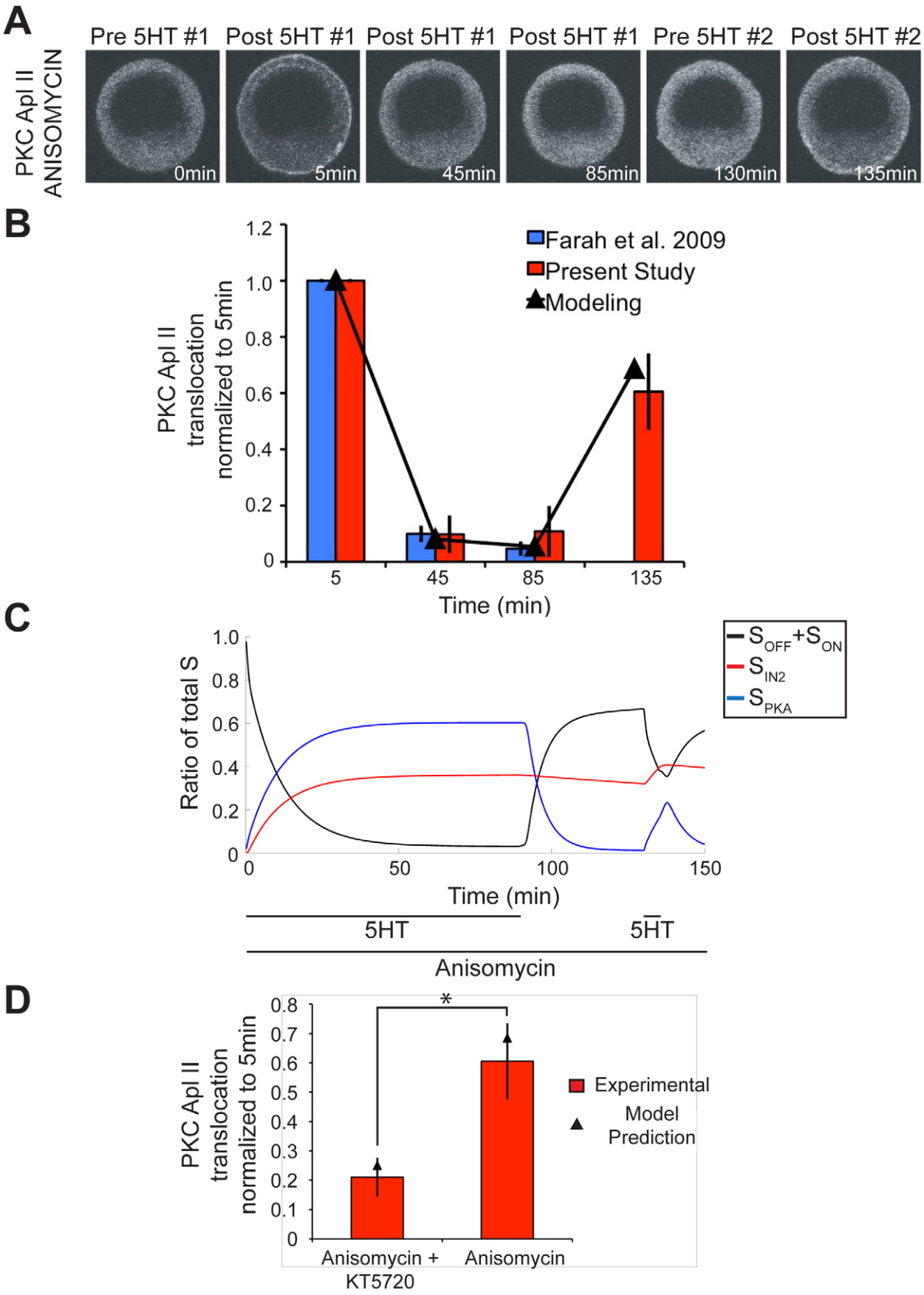
A
PKC Apl II
ANISOMYCIN
Pre 5HT #1
Post 5HT #1
Post 5HT #1
Post 5HT #1
Pre 5HT #2
Post 5HT #2
0min
5min
45min
85min
130min
135min
B
PKC Apl II translocation normalized to 5min
Farah et al. 2009
Present Study
Modeling
Time (min)
C
Ratio of total S
$S_{OFF}+S_{ON}$
S_{IN2}
S_{PKA}
Time (min)
5HT
5HT
Anisomycin
D
PKC Apl II translocation normalized to 5min
Experimental
Model Prediction
Anisomycin + KT5720
Anisomycin

Figure 5. Modeling and experimental validation of desensitization mediated by PKA pathway. A, Representative confocal fluorescence images of sensory neurons expressing eGFP-PKC Apl II during a 90 min exposure to 5HT followed by a 45 min wash and then a 5 min 5HT application, all in the presence of anisomycin. **B**, Quantification of PKC Apl II translocation (bars) and modeling output (line). Blue bars are data used from Farah et al. (2009) to fit the model parameters. Red bars are from the present study (n = 10 cells). **C**, Modeling of S dynamics in response to experimental protocol. Black line represents the ratio of S_{OFF} and S_{ON} to total S, the red line the ratio of S_{IN2} to total S, and the blue line represents ratio of S_{PKA} to total S. **D**, Comparing PKC translocation at 135 min after the second 5HT pulse with PKA inactive (anisomycin and KT5720) and PKA active (anisomycin). Student's unpaired two-tailed T test conducted and statistical significance of $p<0.01$ illustrated by *.
doi:10.1371/journal.pcbi.1002324.g005

Sensitivity analysis

A parameter sensitivity analysis was performed on the completed model to investigate which parameters were most important in driving the results of the model. Each parameter was varied between +/−5% and +/−50% while holding the other parameters at their defined values. The model was then simulated using a 90 min application of 5HT and its resulting PKC Apl II translocation compared to that observed by Farah et al. (2009), which was initially used to fit the model. The sensitivity of a parameter was classified as High if either a +/−5% change in its value caused a change in the fit of the data of over 25%. Similarly, the sensitivity of a parameter was Medium if either a +/−50% change in value caused a change in the fit of the data of over 25%, and Low if the +/−50% change in value did not change the fit by more than 25%. This was then repeated using a spaced application of 5HT (5×5 min 5HT with 15 min washes). The complete sensitivity analysis is summarized in Table 1.

Of the 41 parameters, 5 were classified as High, 12 as Medium, and 6 as Low in both massed and spaced training sensitivity analysis. Interestingly, the majority of the parameters (3/5) with high sensitivity for both types of training were those associated with the initial component of the model responsible for activating PKC Apl II. The remaining two parameters involved how AD works (the synthesis rate and its ability to stop S from going into S_{PKA}). It is not surprising that changing parameters that affect the initial translocation of PKC Apl II by 5HT and its decay after 5HT is removed would have a large effect on the model output, since the model was built around this core. However, these parameters were chosen in a somewhat arbitrary fashion to fit the initial data since the actual rates of DAG synthesis and decay are not known in this system. To ensure that the set of values we chose for these parameters are not critical for the working of the model, we found another parameter set that could fit the initial translocation data (see Table 1). Reassuringly, the rest of the model still worked, suggesting that the model was not dependent on the actual values for these initial parameters, just the ability of the model to replicate the known rate of PKC Apl II translocation and dissociation by 5HT.

The remaining 18 parameters had sensitivities dependent on the type of 5HT application profile. Interestingly, about the same number of parameters had specific high sensitivity for massed (5) vs spaced (4). For spaced, two of these are again from the initial model and the others concern the synthesis rate of D and AD. Similarly, for massed, two of these are for the initial model and the others concern the synthesis rate for D. The sensitivity analysis suggests, similar to the experiments, that the critical parameters that determine the model are involved in the synthesis of D and AD.

Discussion

We have successfully modeled the differences in desensitization of the PKC Apl II response to spaced and massed applications of serotonin. Two major insights were achieved by this modeling. The first was that despite the greater desensitization present with PKA activity present, PKA activity actually protected the ability of 5HT to translocate PKC Apl II at later times due to placing the signaling complex into a state where it could recover. The second insight is that the major determinant of how the system responds to spacing is the production and degradation rate of proteins, suggesting that the production of proteins with short half-lives is a powerful mechanism for cells to be able to sense a time domain in the order of minutes to hours. While this model is probably not unique, its proven ability to predict the results of new experiments suggests that it has captured the essential elements of the biological process it models.

Biological plausibility of the model

The architecture of our model is based on the fact that desensitization and resensitization of GPCRs is due to endocytosis followed by exocytosis, the simplest biological substantiation of the states of S are distinct endocytic recycling pathways of the receptor or distinct states of the receptor after association with GPCR binding-proteins [29,39]. Below we review these processes and the plausibility of the parameters we have assigned to these steps. We also review other aspects of the model and whether the parameters and architecture are biologically plausible.

S_{IN1}, S_{IN2}. S_{IN1} would represent a fast recycling pool, whereas S_{IN2} would represent sorting to lysosomes or other slowly cycling pools (i.e. back to the trans-Golgi network) [40,41]. The rate of S_{ON} to S_{IN1} is less than a minute and similar rates have been seen for internalization of GPCRs using live imaging, suggesting all the steps in this process, including phosphorylation, arrestin binding and endocytosis can occur in less than one minute [22,42]. The back rate S_{IN1} to S_{OFF} is also very fast, less than one minute and this is faster than most measurements for resensitization of GPCRs, where this usually takes minutes [22]; however there are fast recycling pathways from endosomes that do occur in this time range and thus this transition is still plausible [43]. It should also be noted that both S_{ON} to S_{IN1} and S_{IN1} to S_{OFF} rates are part of the initial parameter set, for which we have already found multiple parameter sets that could match the data without changing the overall functioning of the model. S_{IN1} to S_{IN2} has a rate of minutes, which is reasonable for sorting into a late endosome [22,24]. It should be noted that there are multiple steps after the initial sorting event prior to degradation in lysosomes, and actual degradation usually is not seen until hours after internalization [22,24]. The very slow return rate from S_{IN2} is consistent either with slow recycling or degradation [22,24] and we would need to examine much longer recovery times to resolve this issue.

S_{PKA}. S_{PKA} would represent localization to a regulated recycling pool [24]. The rate of heterologous desensitization (S_{OFF} to S_{PKA} - minutes) is consistent with rates observed for heterologous desensitization of other GPCRs [44]. It is known that phosphorylation of receptors or associated proteins can regulate the pool that they are found in [39] and thus the ability of PKA phosphorylation to put the signaling complex into a specific endocytic pool is plausible. Why PKA activity is required for inhibition of the recycling pathway is less obvious. One could envision a receptor binding protein important for recycling whose

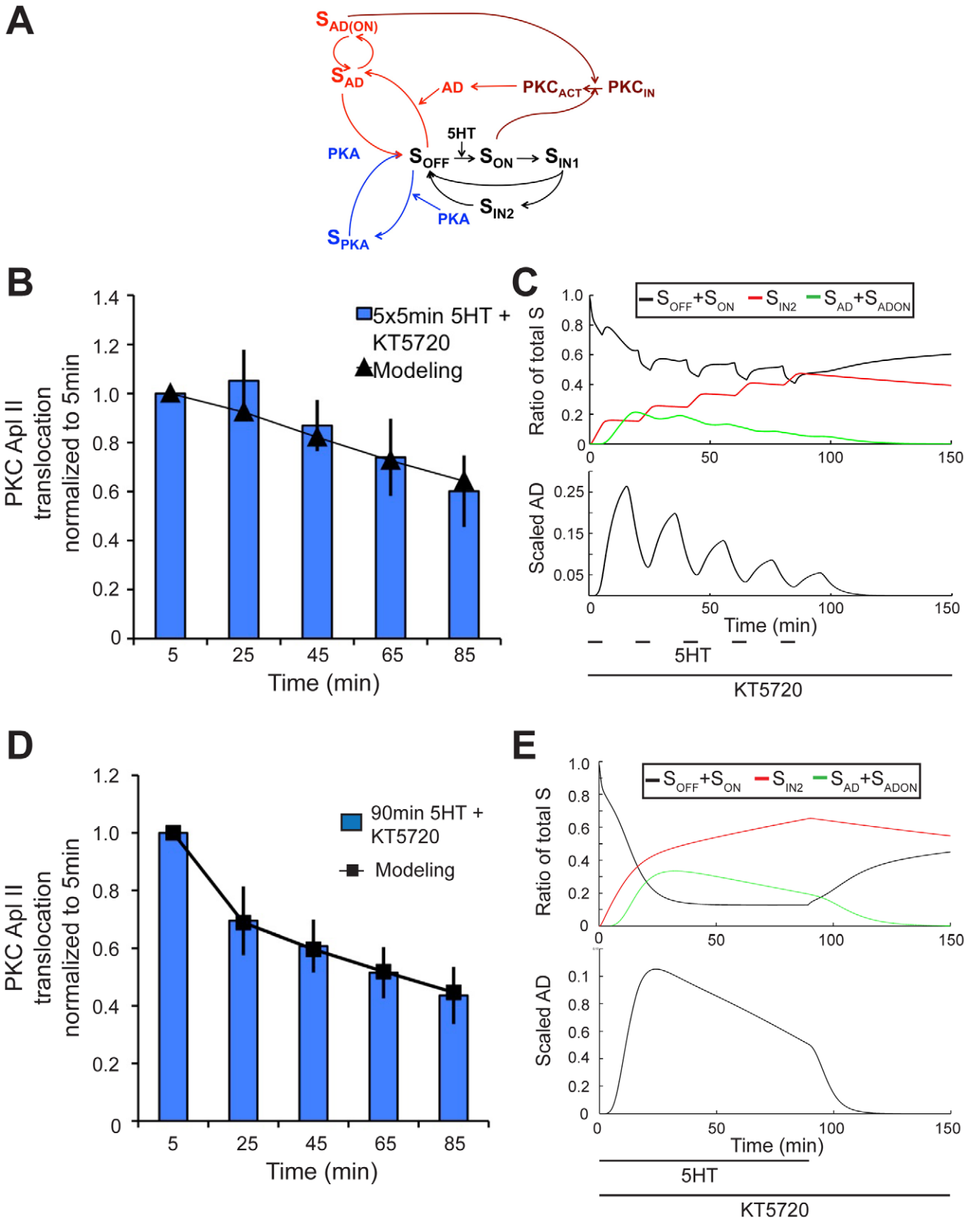

Figure 6. Modeling the rescue from desensitization by Anti-Desensitizer (AD) protein. A, Model network pathways of AD desensitization protection pathway (red network designates AD pathway). **B**, PKC Apl II translocation in response to 5×5 min application of 5HT with 15 min washes in between and KT5720 present throughout from Farah et al. (2009) (bars) and modeling output (line). **C**, Top panel represents S dynamics in response to experimental protocol from **B**. Black line represents the ratio of S_{OFF} and S_{ON} to total S and the red line the ratio of S_{IN2} to total S, and

green line represents the ratio of S_{AD} and S_{ADON} to total S. Bottom panel represents the amount of AD over time. **D**, PKC Apl II translocation in response to 90 min application of 5HT and KT5720 present throughout from Farah et al. (2009) (bars) and modeling output (line). **E**, Top panel represents S dynamics in response to experimental protocol from **D**. Line colours similar to in **C**.
doi:10.1371/journal.pcbi.1002324.g006

ability to bind is blocked by continuous PKA phosphorylation. Alternatively, PKA may regulate vesicular trafficking proteins that regulate the fusion of a storage vesicle with the membrane.

S_{AD}. The AD protein must prevent inactivation, prevent endocytosis and promote faster recycling. It presumably does this by binding to the GPCR. This binding can occur either to S_{OFF} or S_{PKA} and in either case transforms S into S_{AD}. In the model, the requirement for the AD protein to recover the signaling complex from S_{PKA} suggests that the binding is dominant over the PKA site and may be equivalent to the increased recycling seen when PKA is turned off. Presumably the binding of AD would compete with the speculated receptor binding protein important for retaining the signaling complex in a PKA sensitive pool as well as prevent cycling into S_{IN2}. A number of proteins have been identified that can both retain GPCRs on the membrane and speed recycling of GPCRs, mostly PDZ proteins that bind to the carboxy-terminus of receptors, and these would be candidates for AD [39,45]. Interestingly PDZ proteins such as PSD-95 have been shown to be targets of fast synthesis and degradation [46,47].

Our model makes strong predictions concerning AD that will be useful to ascertain the true identity of the AD protein. We predict that over expression of the protein would be sufficient to prevent desensitization. Furthermore, we predict that the protein should bind directly to the GPCR that is responsible for PKC activation. In the future, it will be interesting to test orthologues of these PDZ proteins in *Aplysia* to identify binding partners to the GPCR that have these properties.

The slow rate of S_{AD} to S_{OFF} is surprising, as one would expect this rate to be fast once AD is degraded. It is possible that the AD bound to the receptor degrades more slowly than the free pool of AD. If AD was a PDZ domain-containing protein, the off rate of PDZ proteins can be quite slow [48]. It should also be noted that the S_{PKA} to S_{AD} rate is slower than the S_{OFF} to S_{AD} rate. Since both rates may involve binding of AD to the receptor, one might expect them to be the same. However, since S_{OFF} and S_{PKA} may represent separate compartments, the availability of AD could be different. It is also possible that AD is slower to bind the phosphorylated receptor than the non-phosphorylated receptor.

D. The D protein promotes the movement of the complex into the regulated recycling compartment. One protein that would be a candidate for this would be the clathrin light chain that is known to be translationally produced downstream of PKA in sensory neurons [49] and is associated with target-specific clathrin-mediated endocytosis events [50,51]. Since D mainly increases the ability of PKA to move S into S_{PKA}, it would be consistent for D to be PKA itself or a protein involved in increasing activation of PKA. However, while there is a protein-synthesis dependent activation of PKA after spaced training [10], this is not observed until after 4 or 5 pulses of 5HT, while D has a major effect after a single pulse of 5HT. The amount of PKA activation is not different after the second or third pulse compared to the first pulse [10].

Speed of protein synthesis and degradation. The model predicts that proteins are produced and degraded quite quickly, in a time scale of minutes. The fast rate of protein production for proteins involved in plasticity is becoming more widely accepted. In mGLUR-LTD in hippocampal neurons, levels of Arc are significantly increased 5 min after treatment [52]. In *Aplysia*, protein synthesis is required for plasticity after 5HT as soon as 5 minutes after training or 5HT application [53,54]. The degradation rates of the proteins are also fast, but not inconsistent with other plasticity related proteins such as Arc whose half-life appears to be on the order of minutes [55,56]. The delay in production of D could be biologically caused by a number of different models. One possibility is in the delayed activation of the translation factors required for initiation. A larger protein will have a longer lag between initiation and production of protein. There may be a cascade of factors involved and perhaps translation of an additional protein is required to initiate translation of D. While the model puts the lag in the production of D, it may be that after production D requires time to act, either due to a requirement for posttranslational modification, or transport to an important site. This would lead to an equivalent delay.

Integrals, thresholds, and Hill functions. It was important to allow AD protein to be synthesized during massed, but not spaced, applications of 5HT, as discussed above. This required us to differentiate the amount of time that PKC Apl II was activated (longer in massed, than in spaced). We accomplished this by integrating PKC Apl II activity over time and then applying a Hill function in order to generate a threshold of PKC Apl II activity that would lead to AD synthesis. We also used Hill functions in a number of other steps (D synthesis and transforming or inhibiting the transformation of S into its different states) as they are well-behaved mathematical functions that are widely used in biological modeling, especially when a nonlinear saturating dynamic is desired and there is limited biological information on the actual mechanisms underlying step or when multiple reactions are modeled in one step [57].

Comparison to other models that explain timing during plasticity

Spaced vs. massed training occurs in a number of different time scales, thus molecular mechanisms are required that act in different time domains. For example, induction of LTP by spaced stimuli requires PKA, but not when massed stimulation is used [58], and the spaced stimuli were required to recruit protein synthesis-dependent mechanism [59]. A recent model explains this finding based on the differential effects of calcium on PKA and CAMKII. This model depends on inter-trial intervals that range between seconds and 5 minutes [60]. The frequency dependent activation of CAMKII is sensitive to timing intervals in this period and is proposed to be the mechanism for sensing the spacing between stimuli [61]. In mice object recognition was enhanced by spacing of 15 min, compared to 5 min or massed training [62]. In mice that lacked Protein Phosphatase 1 (PP1), 5 min spacing was sufficient for learning. In this case the rate-limiting step for learning was activation of CREB, and spacing was required in order for PP1 to be deactivated before the next training trial allowing for CREB activation [62]. CREB activation is also the proposed difference between spaced and massed learning in *Drosophila* odor avoidance [63]. In *Drosophila*, spacing is regulated by waves of MAP kinase activation where both the activation and decay kinetics appear critical for the spacing interval [64]. In *Aplysia*, it has recently been demonstrated that for long-term facilitation, only two spaced trials are required, 45 minutes apart, but neither 30 nor 60 minute spacing is adequate [65]. Again, in this case the spacing corresponds to a wave of MAP kinase

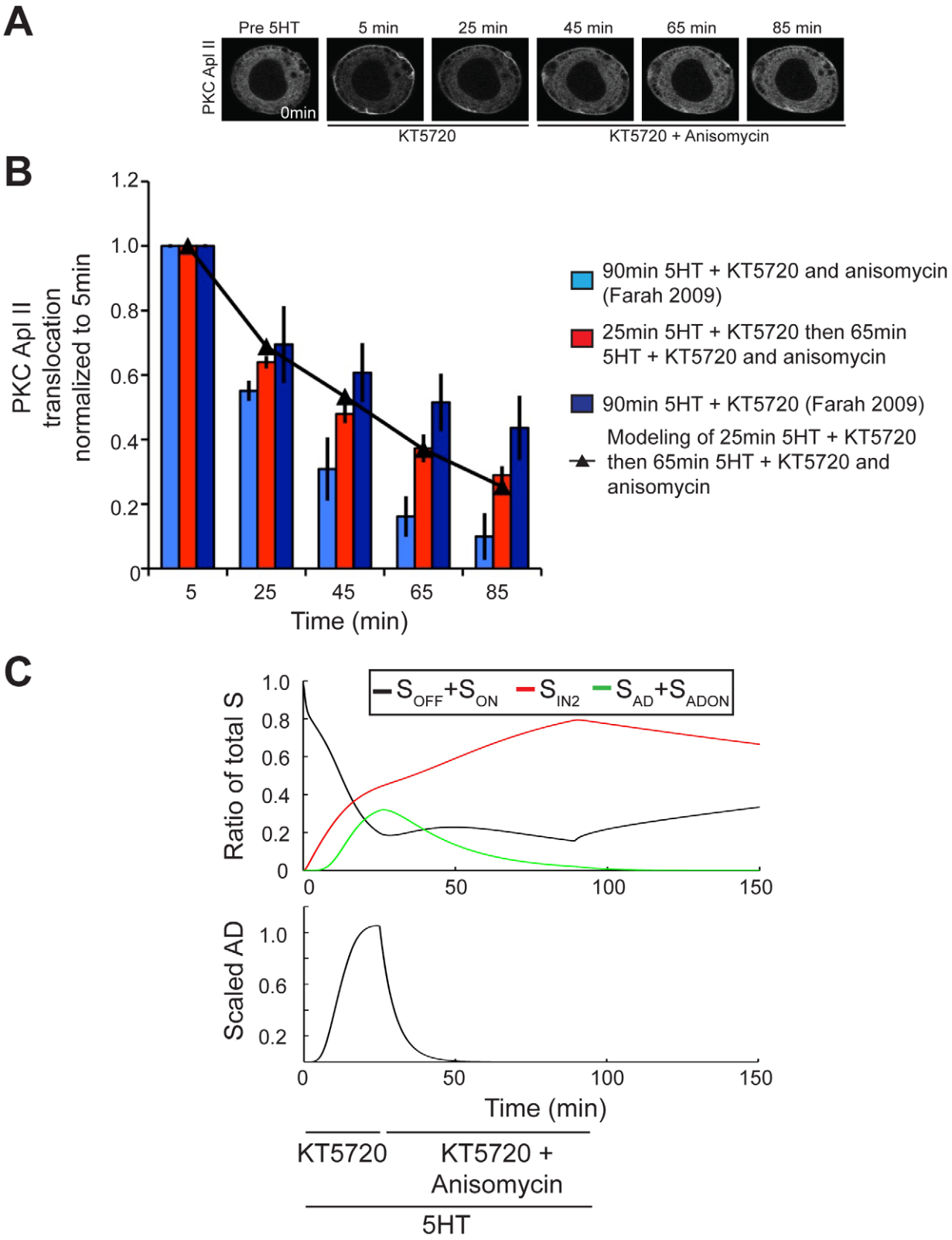

Figure 7. Experimental validation of AD dynamics. A, Representative confocal fluorescence images of sensory neurons expressing eGFP-PKC Apl II during a 90 min exposure to 5HT where during the first 25 min KT5720 alone was applied, while during the last 40 min both anisomycin and KT5720 was applied. **B**, Quantification of PKC Apl II translocation (bars) and modeling output (line with square points). 90 min 5HT with KT5720 and anisomycin (light blue bars) is similar to that shown in Figure 1C and 90 min 5HT with anisomycin (dark blue bars) is similar to that shown in Figure 4D. These data points, from Farah et al. (2009), are reproduced here for comparison purposes with the following newly acquired data. Error bars are SEM. Red bars represent quantification of eGFP-PKC Apl II translocation during experimental protocol from **A** (n = 9 cells) compared to line

with triangles for the modeling prediction of this experimental protocol (25 min 5HT with KT5720 followed by 65 min with KT5720 and ansiomycin). **F**, Top panel represents S dynamics in response to experimental protocol from **D**. Black line represents the ratio of S_{OFF} and S_{ON} to total S and the red line the ratio of S_{IN2} to total S, and green line represents the ratio of S_{AD} and S_{ADON} to total S. Bottom panel represents the amount of AD over time.
doi:10.1371/journal.pcbi.1002324.g007

activation [65]. None of these cases directly implicate the rates of protein synthesis or degradation as critical for timing, although it is possible that the induction of MAP kinase activation at later times may require protein synthesis. Interestingly, the activation of CREB in mammals appears to require removal of CREB repressor, which requires both blockade of translation through eIF2a dephosphorylation [66] and increased degradation due to proteosomal activation [67]. Thus, in this case regulating the level of a protein also may mediate differences between spaced and massed trained determining whether or not transcription is activated. It will be interesting in the future to determine how generally neurons sense time through measuring the half-life of newly synthesized proteins.

Materials and Methods

Mathematical modeling

A mathematical model of the desensitization of PKC Apl II translocation in *Aplysia californica* sensory neurons was constructed in the MATLAB programming environment. The model consists of a system of integro-differential equations with delays, where each equation describes the change in concentration of the proteins PKC Apl II, PKA, Desensitizer (D), Anti-Desensitizer (AD), and of each instance of the signaling complex (S). Since we are only interested in PKC Apl II translocation occurring between the cytosol and plasma membrane [18] a single compartment model was used.

The complete model is depicted in Figure 2. The colours of this figure correspond to the components of the model. The model was constructed in a sequential manner. First, the components outlined in black and maroon were fit to data [13] at which point its parameters were specified and not allowed to change. Following these component's completion, the component outlined in blue was similarly constructed, then the red component and finally the green component. In order to illustrate this sequential construction within the model equations, we have named the parameters according to which component they reside in: A for the black component, B for blue, C for red, and D for green.

The most basic component of the model is the translocation of PKC Apl II from the cytosol to the plasma membrane (maroon component). This translocation is proportional to the concentration of diacylglycerol (DAG) on the membrane and thus the translocation is given by the following equation:

$$\frac{d}{dt}PKC = k_{DAGp}\cdot(S_{ON}+S_{ADON}) - k_{DAGd}\cdot PKC, \qquad (1)$$

where k_{DAGp} is the rate of PKC Apl II translocation to the membrane, and k_{DAGd} the rate of PKC Apl II removal from the membrane. S_{ON} represents the proportion of S currently in the active state, which is capable of translocating PKC Apl II to the membrane. The inactive state of S is given by S_{OFF}, and S_{IN1} is a transition state between S_{ON} and S_{OFF}. S can be transformed into 3 other states, as will be described next. We require the total amount of S to remain constant by employing the following restriction: $\sum_i S_i = S_{TOT}$, where i = ON, OFF, IN1, IN2, PKA, AD, and D. We scale each S variable by $1/S_{TOT}$, such that all parameters k_i, i = A1–A5, B1–B2, C1–C2, and D1–D3 will have units min^{-1}. We have set $S_{TOT} = 1$, where we refrain from assigning units to the S variables since we cannot measure the concentrations of PKA or PKC in *Aplysia* neurons in order to accurately define a unit of measure. Furthermore, units are not assigned to any variable with concentration as a possible dimension. This simplification is justified since we have developed a single compartment model of *Aplysia* sensory neurons to qualitatively describe the dynamics of PKC desensitization. Using non-dimensional variables and parameters allows us to observe important dynamics, such as relative magnitudes of proteins and the time course of S recycling, which allow us to gain insight into the molecular regulatory mechanism involved in the desensitization of PKC translocation.

The following equations describe the rates of change of concentration of the first four S states:

$$\frac{d}{dt}S_{ON} = k_{A1}\cdot[5HT]\cdot S_{OFF} - k_{A2}\cdot S_{ON}, \qquad (2)$$

$$\begin{aligned}\frac{d}{dt}S_{OFF} = {} & -k_{A1}\cdot[5HT]\cdot S_{OFF} + k_{A3}\cdot S_{IN1} + k_{A5}\cdot S_{IN2} + \\ & k_{B2}\cdot S_{PKA}\cdot\frac{k_{B2a}{}^{k_{B2b}}}{(k_{B2a}{}^{k_{B2b}} + PKA^{k_{B2b}})}\cdot\frac{k_{D2a}{}^{k_{D2b}}}{(k_{D2a}{}^{k_{D2b}} + D^{k_{D2b}})} \\ & -k_{C1}\cdot S_{OFF}\cdot AD + k_{C2}\cdot S_{AD}\cdot\frac{k_{C2a}{}^{k_{C2b}}}{k_{C2a}{}^{k_{C2b}} + AD^{k_{C2b}}} - \\ & (k_{B1}\cdot PKA + k_{D1}\cdot D)\cdot S_{OFF}\cdot\frac{k_{D1a}{}^{k_{D1b}}}{k_{D1a}{}^{k_{D1b}} + AD^{k_{D1b}}},\end{aligned} \qquad (3)$$

$$\frac{d}{dt}S_{IN1} = k_{A2}\cdot S_{ON} - (k_{A3}+k_{A4})\cdot S_{IN1}, \qquad (4)$$

$$\frac{d}{dt}S_{IN2} = k_{A4}\cdot S_{IN1} - k_{A5}\cdot S_{IN2}, \qquad (5)$$

where [5HT] represents the concentration of 5HT being applied to the system and is given a standard value of 10 μM during any application of 5HT, k_{A1} represents the transformation of S_{OFF} into S_{ON}, k_{A2} of S_{ON} into S_{IN1}, k_{A3} of S_{IN1} into S_{OFF}, k_{A4} of S_{IN1} into S_{IN2}, and k_{A5} of S_{IN2} into S_{OFF}. The additional terms in equation (3) refer to the further transformations that S_{OFF} can undergo. Without these additional terms these equations describe the black model in Figure 3A. The first additional transformation of S_{OFF} is mediated by the catalytic subunit of PKA, where S_{OFF} is converted to S_{PKA}, which has the following equation:

$$\begin{aligned}\frac{d}{dt}S_{PKA} = {} & (k_{B1}\cdot PKA + k_{D1}\cdot D)\cdot S_{OFF}\cdot\frac{k_{D1a}{}^{k_{D1b}}}{k_{D1a}{}^{k_{D1b}} + AD^{k_{D1b}}} - \\ & k_{B2}\cdot S_{PKA}\cdot\frac{k_{B2a}{}^{k_{B2b}}}{(k_{B2a}{}^{k_{B2b}} + PKA^{k_{B2b}})}\cdot\frac{k_{D2a}{}^{k_{D2b}}}{(k_{D2a}{}^{k_{D2b}} + D^{k_{D2b}})} \\ & -k_{D3}\cdot S_{PKA}\cdot\frac{AD^{k_{D3b}}}{k_{D3a} + AD^{k_{D3b}}},\end{aligned} \qquad (6)$$

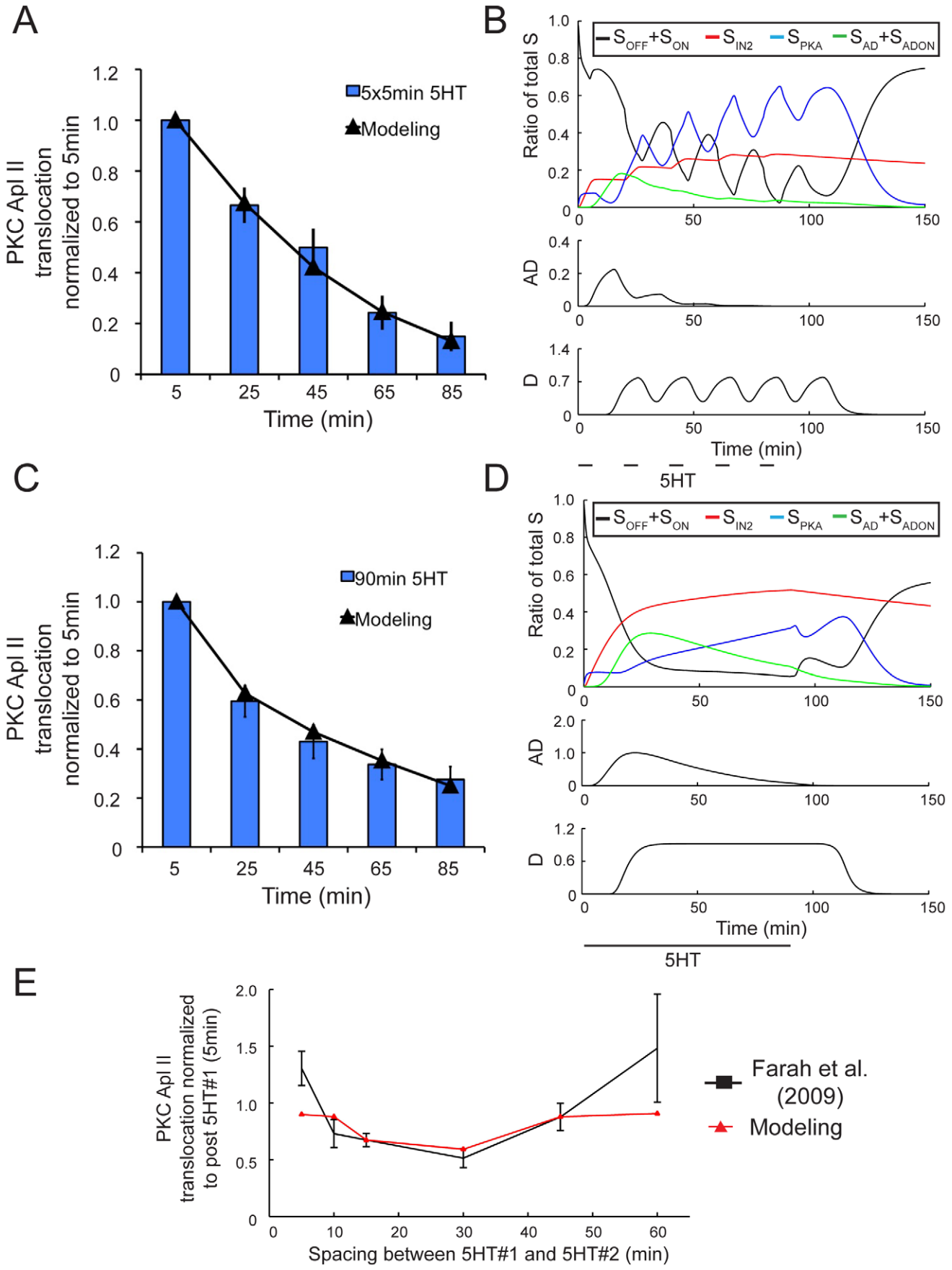
A
PKC Apl II translocation normalized to 5min
5x5min 5HT
Modeling
Time (min)
B
Ratio of total S
$S_{OFF}+S_{ON}$
S_{IN2}
S_{PKA}
$S_{AD}+S_{ADON}$
AD
D
Time (min)
5HT
C
PKC Apl II translocation normalized to 5min
90min 5HT
Modeling
Time (min)
D
Ratio of total S
$S_{OFF}+S_{ON}$
S_{IN2}
S_{PKA}
$S_{AD}+S_{ADON}$
AD
D
Time (min)
5HT
E
PKC Apl II translocation normalized to post 5HT#1 (5min)
Farah et al. (2009)
Modeling
Spacing between 5HT#1 and 5HT#2 (min)

Figure 8. Fitting complete model to PKC translocation measured during no pharmacological interventions. A, PKC Apl II translocation in response to 5×5 min application of 5HT with 15 min washes in between (bars) and modeling output (line). **B**, Top panel represents S dynamics in response to experimental protocol from **A**. Black line represents the ratio of S_{OFF} and S_{ON} to total S, red line the ratio of S_{IN2} to total S, green line represents the ratio of S_{AD} and S_{ADON} to total S, and blue line represents the ratio of S_{AD} and S_{ADON} to total S. Middle panel is the amount of AD over time and the bottom panel is the amount of D over time. **C**, PKC Apl II translocation in response to a 90 min application of 5HT (bars) and modeling output (line). **D**, Top panel represents S dynamics in response to experimental protocol from **G**, with line colours identical to in **B**. Middle panel represents the amount of AD over time and the bottom panel the amount of D over time. **E**, PKC Apl II translocation in response to 2×5 min applications of 5HT with varying wash periods in between (black line) and modeling output (red line).
doi:10.1371/journal.pcbi.1002324.g008

where k_{B1} is rate constant of the transformation from S_{OFF} into S_{PKA}, which is brought about by the activity of the catalytic subunit of PKA or the protein D. However, the protein AD, through a Hill function with coefficient k_{D1b} and half saturation k_{D1a}, can inhibit this conversion. The recycling of S_{PKA} into S_{OFF} occurs with rate constant k_{B2}, but is inhibited by PKA and D through inhibiting Hill functions with coefficients k_{B2b} and k_{D2b}, respectively, and half saturations k_{B2a} and k_{D2a}, respectively. Also, activity of AD can convert S_{PKA} into S_{AD} with a rate constant k_{D3} and a Hill function with coefficient k_{D3b} and half saturation k_{D3a}.

The dynamics of the catalytic and regulatory subunits of PKA are adapted from a model presented by Pettigrew et al. (2005), where the changes to this model are described in the results. PKA dynamics are given in the following equations:

$$\frac{d}{dt}cAMP = V_m \frac{[5HT]}{k_{5HT}+[5HT]} - (cAMP - cAMP_{basal}), \quad (7)$$

$$\frac{d}{dt}R = K_{fpka}\cdot RC\cdot cAMP^2 - K_{bpka}\cdot R\cdot C, \quad (8)$$

$$\frac{d}{dt}C = K_{fpka}\cdot RC\cdot cAMP^2 - K_{bpka}\cdot R\cdot C, \quad (9)$$

$$\frac{d}{dt}RC = -K_{fpka}\cdot RC\cdot cAMP^2 + K_{bpka}\cdot R\cdot C, \quad (10)$$

Where V_m is the cAMP synthesis rate constant, and K_{5HT} is the half saturation of the Hill function associated with cAMP synthesis. K_{fpka} is the rate constant associated with the dissociation of the catalytic and regulatory subunits, while the reassociation rate is given by K_{bpka}. The amount of PKA activity is set equal to the amount of the free catalytic subunit (C); PKA = C. The parameters associated with protein synthesis are given the subscript S to differentiate them from signaling complex dynamics. The synthesis of AD and D are given by the following equations:

$$\frac{d}{dt}AD = k_{S1}\cdot \frac{f(PKC,t)^{k_{S1b}}}{k_{S1a}{}^{k_{S1b}} + f(PKC,t)^{k_{S1b}}} - k_{S2}\cdot AD, \quad (11)$$

$$f(PKC,t) = \int_{t-\mathrm{int}\,PKC}^{t} PKC(t)\cdot dt, \quad (12)$$

$$\frac{d}{dt}D = k_{S3}\cdot \frac{g(PKA,t)^{k_{S3b}}}{k_{S3a}{}^{k_{S3b}} + g(PKA,t)^{k_{S3b}}} - k_{S4}\cdot D, \quad (13)$$

$$g(PKA,t) = \int_{t-\mathrm{int}\,PKA}^{t} PKA(t-delayD)\cdot dt, \quad (14)$$

AD synthesis depends on the total activity of PKC Apl II over a previous time window of duration given by intPKC in equation (12). The integration of PKC Apl II activity leads to the synthesis of AD through a Hill function with coefficient k_{S1b} and half saturation k_{S1a}. k_{S2} represents the AD degradation constant. Similarly, D synthesis depends on an integration of PKA activity over a time period of intPKA in equation (14), which leads to the synthesis of D with a rate constant of k_{S3} and through a Hill function with coefficient k_{S3b} and half saturation k_{S3a}. The degradation of D is given by rate constant k_{S4}. D leads to the transformation of S_{OFF} into S_{PKA}, which was described above in equation (6), while AD transforms S_{OFF} into S_{AD}, whose dynamics are modeled with the following equation:

$$\frac{d}{dt}S_{AD} = k_{C1}\cdot S_{OFF}\cdot AD - k_{A1}\cdot[5HT]\cdot S_{AD} + k_{A2}\cdot S_{ADON} - k_{C2}\cdot S_{AD}\cdot \frac{k_{C2a}{}^{k_{C2b}}}{k_{C2a}{}^{k_{C2b}} + AD^{k_{C2b}}} + k_{D3}\cdot S_{PKA}\cdot \frac{AD^{k_{D3b}}}{k_{D3a}{}^{D3b} + AD^{k_{D3b}}}, \quad (15)$$

where k_{C1} is the rate constant associated with the transformation of S_{OFF} into S_{AD}, k_{C2} the rate constant of the recycling of S_{AD} into S_{OFF}, which can be inhibited by AD through a Hill function with coefficient k_{C2b} and half saturation k_{C2a}. Also, S_{AD} can become activated when 5HT transforms it into S_{ADON}, whose dynamics are given in the following equation:

$$\frac{d}{dt}S_{ADON} = k_{A1}\cdot[5HT]\cdot S_{AD} - k_{A2}\cdot S_{ADON}, \quad (16)$$

whose transformation and recycling rate constants are identical to those of S_{OFF} into S_{ON}. S_{ADON} activates PKC Apl II in an identical fashion to S_{ON} in equation (1).

The system was solved numerically by employing a 4th order Runga-Kutta scheme to solve the differential equations and the Trapezoid Rule to solve the integrals [68]. Parameter estimation was conducted with the help of the MATLAB Optimization Toolbox and Global Optimization Toolbox, specifically the functions lsqcurvefit, ga, and fmincon. These functions were used to minimize the least squares distance between the modeling output and experimental data. Values of individual parameters are given in Table 1.

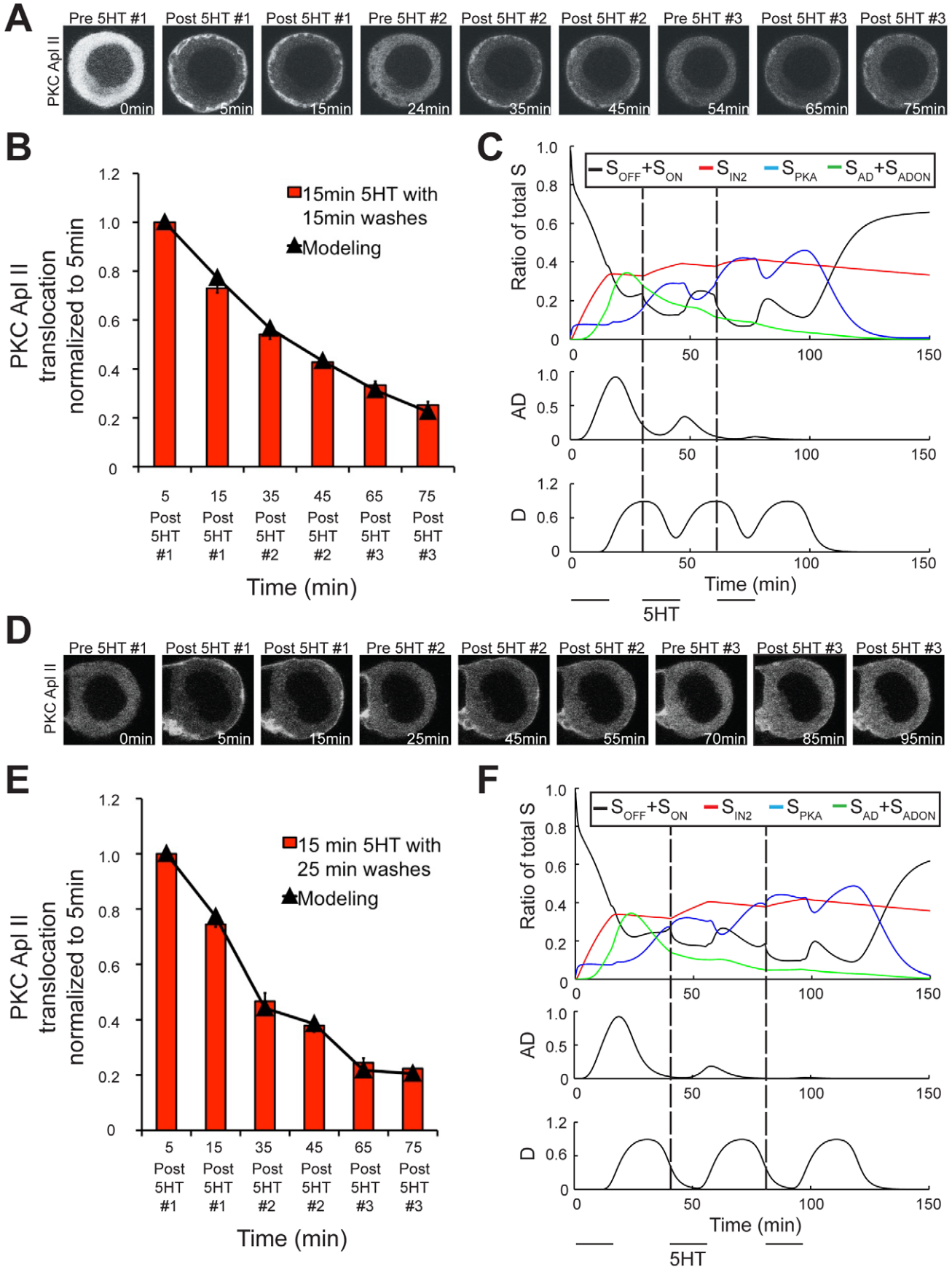
A
Pre 5HT #1
Post 5HT #1
Post 5HT #1
Pre 5HT #2
Post 5HT #2
Post 5HT #2
Pre 5HT #3
Post 5HT #3
Post 5HT #3
PKC Apl II
0min
5min
15min
24min
35min
45min
54min
65min
75min
B
PKC Apl II translocation normalized to 5min
15min 5HT with 15min washes
Modeling
5 Post 5HT #1
15 Post 5HT #1
35 Post 5HT #2
45 Post 5HT #2
65 Post 5HT #3
75 Post 5HT #3
Time (min)
C
S_OFF+S_ON
S_IN2
S_PKA
S_AD+S_ADON
Ratio of total S
AD
D
Time (min)
5HT
D
Pre 5HT #1
Post 5HT #1
Post 5HT #1
Pre 5HT #2
Post 5HT #2
Post 5HT #2
Pre 5HT #3
Post 5HT #3
Post 5HT #3
PKC Apl II
0min
5min
15min
25min
45min
55min
70min
85min
95min
E
PKC Apl II translocation normalized to 5min
15 min 5HT with 25 min washes
Modeling
5 Post 5HT #1
15 Post 5HT #1
35 Post 5HT #2
45 Post 5HT #2
65 Post 5HT #3
75 Post 5HT #3
Time (min)
F
S_OFF+S_ON
S_IN2
S_PKA
S_AD+S_ADON
Ratio of total S
AD
D
Time (min)
5HT

Figure 9. Longer wash periods lead to greater desensitization of PKC Apl II translocation. A, Representative confocal fluorescence images of sensory neurons expressing eGFP-PKC Apl II during a 3×15 min application of 5HT with 15 min washes in between. **B**, Quantification of PKC Apl II translocation (bars, n = 9 cells) and modeling output (line). Error bars are SEM. **C**, Top panel represents S dynamics in response to experimental protocol from **A**. Black line represents the ratio of S_{OFF} and S_{ON} to total S, red line the ratio of S_{IN2} to total S, green line represents the ratio of S_{AD} and S_{ADON} to total S. Middle panel represents the amount of AD over time and the bottom panel the amount of D over time. Dotted line represents time of second and third 5HT application. **D**, Representative confocal fluorescence images of sensory neurons expressing eGFP-PKC Apl II during a 3×15 min applications of 5HT with 25 min washes in between. **E**, Quantification of PKC translocation (bars, n = 6 cells) and modeling output (line). Error bars are SEM. **F**, Top panel represents S dynamics in response to experimental protocol from **E**. Black line represents the ratio of S_{OFF} and S_{ON} to total S, red line the ratio of S_{IN2} to total S, green line represents the ratio of S_{AD} and S_{ADON} to total S. Dotted line represents time of second and third 5HT application. Middle panel represents the amount of AD over time and the bottom panel the amount of D over time.
doi:10.1371/journal.pcbi.1002324.g009

Aplysia cell culture preparation

Adult *Aplysia californica* (76 to 100 g; University of Miami *Aplysia* Resource Facility, RSMAS, FL) organisms were anesthetized by an injection of 50 to 100 ml of 400 mM (isotonic) MgCl2. Pleuropedal ganglia were removed and digested in L15 medium containing 1% protease type IX (Sigma). L15 medium was purchased from Sigma and supplemented with 0.2 M NaCl, 26 mM MgSO4·7H2O, 35 mM dextrose, 27 mM MgCl2·6H2O, 4.7 mM KCl, 2 mM NaHCO3, 9.7 mM CaCl2·2H2O, 15 mM HEPES, and the pH was adjusted to 7.4. Following digestion, tail sensory neurons were isolated and plated in L15 medium containing 50% *Aplysia* hemolymph on MatTek glassbottom culture dishes (MatTek Corporation, Ashland, MA) with a glass surface of 14 mm and a coverslip thickness of 0.085 to 0.13 mm. The dishes were pretreated with poly-L-lysine (molecular weight, >300,000; Sigma).

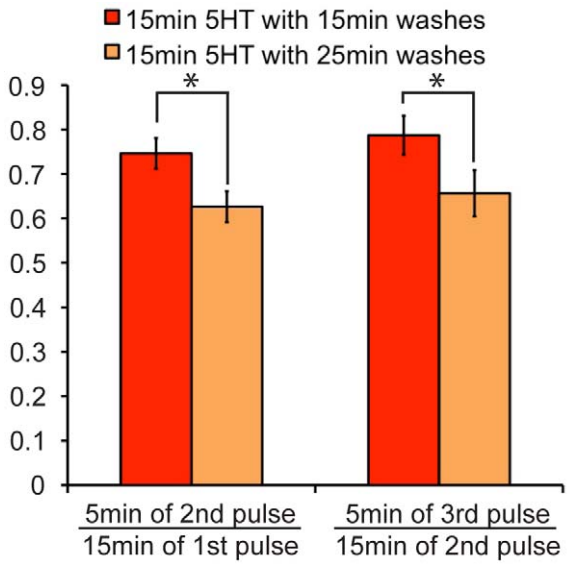

Figure 10. Quantifying the amount of desensitization of PKC Apl II translocation occurring during wash periods. Left pair of bars represent the amount of PKC Apl II translocation at the 5 min point of the second pulse divided by the amount of PKC Apl II translocation at the 15 min point of the first pulse. Right pair of bars represents the amount of PKC Apl II translocation at the 5 min point of the third pulse divided by the amount of PKC Apl II translocation at the 15 min point of the second pulse. Red bars correspond to 15 min 5HT with 15 min washes (n = 9) and Orange to 15 min 5HT with 25 min washes (n = 6). Student's unpaired two-tailed T test conducted and statistical significance of $p<0.05$ illustrated by *.
doi:10.1371/journal.pcbi.1002324.g010

Plasmid construction and microinjection of plasmid vectors

The pNEX3 enhanced green fluorescent protein (eGFP) PKC Apl II has been described previously [13,19,69]. On day 1 after isolation, solutions of plasmids in distilled water containing 0.25% fast green were microinjected into neurons from back-filled glass micropipettes. The tip of the micropipette was inserted into the cell nucleus, and short pressure pulses (10–50 ms duration; 20 lb/in2) were delivered until the nucleus became uniformly green. The cells were incubated for 4–5 hrs at room temperature and then kept at 4°C until use.

Confocal microscopy of Aplysia neurons

Neurons expressing eGFP-PKC Apl II were imaged on a Zeiss laser-scanning microscope (Zeiss, Oberkochen, Germany) with an Axiovert 200 and a ×40 or ×63 oil immersion objective with a 25-mW argon laser with 25% laser output. The laser line was attenuated to 4% transmission output prior to live imaging. 5HT (10 μM) was added to the dish in L15 medium containing 50% hemolymph. 5HT was washed away with artificial seawater (ASW; 10 mM HEPES, pH 7.5, 0.46 M NaCl, 10 mM KCl, 11.2 mM CaCl2·2H2O, 55 mM MgCl2·6H2O). For spaced training, neurons received five applications of 10 μM 5HT (5 min each) at an intertrial interval (ITI) of 20 min. For massed training, neurons received a single continuous application of 10 μM 5HT for 90 min. All experiments were performed at room temperature (20 to 23°C).

Drug treatment

Anisomycin (Sigma-Aldrich), and KT5720 (Calbiochem) were used at concentrations of 50 μM, and were present in the media throughout spaced or massed training. There was no pre-incubation with these drugs prior to 5HT treatment and because of this we erred on the high side of the concentrations that have been used previously. The controls used in all experiments were always performed from the same batch of animals when the drugs were used. The translation inhibitor anisomycin was purchased from Sigma-Aldrich.

Image analysis

The level of PKC Apl II translocation for each cell was determined by tracing three rectangles at random locations at the plasma membrane and three rectangles at random locations in the cytosol. The width of the membrane rectangles was three-five pixels wide to avoid cytoplasmic contamination, but otherwise the size of the rectangles was not constrained. The average intensity at the membrane (Im) and the average intensity in the cytosol (Ic) was then calculated and the Im/Ic ratio is the degree of membrane association. In all figures, the control used to normalize the translocations in the presence of a drug is the post 5HT #1 in the presence of that drug.

Acknowledgments

We thank Edward Ruthazer for his helpful comments.

Author Contributions

Conceived and designed the experiments: FN WSS. Performed the experiments: FN CAF. Analyzed the data: FN CAF CCP WSS. Contributed reagents/materials/analysis tools: FN CAF WSS. Wrote the paper: FN WSS CAF CCP.

References

1. Cepeda NJ, Pashler H, Vul E, Wixted JT, Rohrer D (2006) Distributed practice in verbal recall tasks: A review and quantitative synthesis. Psychol Bull 132: 354–380.
2. Philips GT, Carew TJ (2009) It's all about timing. Cell 139: 23–25.
3. Sutton MA, Ide J, Masters SE, Carew TJ (2002) Interaction between amount and pattern of training in the induction of intermediate- and long-term memory for sensitization in aplysia. Learn Mem 9: 29–40.
4. Kandel ER (2001) The molecular biology of memory storage: a dialogue between genes and synapses. Science 294: 1030–1038.
5. Glanzman DL, Mackey SL, Hawkins RD, Dyke AM, Lloyd PE, et al. (1989) Depletion of serotonin in the nervous system of Aplysia reduces the behavioral enhancement of gill withdrawal as well as the heterosynaptic facilitation produced by tail shock. J Neurosci 9: 4200–4213.
6. Marinesco S, Kolkman KE, Carew TJ (2004) Serotonergic modulation in aplysia. I. Distributed serotonergic network persistently activated by sensitizing stimuli. J Neurophysiol 92: 2468–2486.
7. Mauelshagen J, Sherff CM, Carew TJ (1998) Differential induction of long-term synaptic facilitation by spaced and massed applications of serotonin at sensory neuron synapses of Aplysia californica. Learn Mem 5: 246–256.
8. Lee YS, Choi SL, Lee SH, Kim H, Park H, et al. (2009) Identification of a serotonin receptor coupled to adenylyl cyclase involved in learning-related heterosynaptic facilitation in Aplysia. Proc Natl Acad Sci U S A 106: 14634–14639.
9. Nagakura I, Dunn TW, Farah CA, Heppner A, Li FF, et al. (2010) Regulation of protein kinase C Apl II by serotonin receptors in Aplysia. J Neurochem 115: 994–1006.
10. Muller U, Carew TJ (1998) Serotonin induces temporally and mechanistically distinct phases of persistent PKA activity in Aplysia sensory neurons. Neuron 21: 1423–1434.
11. Sutton MA, Carew TJ (2000) Parallel molecular pathways mediate expression of distinct forms of intermediate-term facilitation at tail sensory-motor synapses in Aplysia. Neuron 26: 219–231.
12. Sossin WS (1997) An autonomous kinase generated during long-term facilitation in Aplysia is related to the Ca(2+)-independent protein kinase C Apl II. Learn Mem 3: 389–401.
13. Farah C, Weatherill D, Dunn T, Sossin W (2009) PKC differentially translocates during spaced and massed training in Aplysia. J Neurosci 29: 10281.
14. Jin I, Kandel ER, Hawkins RD (2011) Whereas short-term facilitation is presynaptic, intermediate-term facilitation involves both presynaptic and postsynaptic protein kinases and protein synthesis. Learn Mem 18: 96–102.
15. Sossin WS, Sacktor TC, Schwartz JH (1994) Persistent activation of protein kinase C during the development of long-term facilitation in Aplysia. Learn Mem 1: 189–202.
16. Sutton M, Ide J, Masters S, Carew T (2002) Interaction between amount and pattern of training in the induction of intermediate-and long-term memory for sensitization in Aplysia. Learn Mem 9: 29.
17. Hu JY, Wu F, Schacher S (2006) Two signaling pathways regulate the expression and secretion of a neuropeptide required for long-term facilitation in Aplysia. J Neurosci 26: 1026.
18. Farah C, Nagakura I, Weatherill D, Fan X, Sossin W (2008) Physiological role for phosphatidic acid in the translocation of the novel protein kinase C Apl II in Aplysia neurons. Mol Cell Biol 28: 4719.
19. Zhao Y, Leal K, Abi-Farah C, Martin K, Sossin W, et al. (2006) Isoform specificity of PKC translocation in living Aplysia sensory neurons and a role for Ca2+-dependent PKC APL I in the induction of intermediate-term facilitation. J Neurosci 26: 8847.
20. Sossin WS (2007) Isoform specificity of protein kinase Cs in synaptic plasticity. Learn Mem 14: 236–246.
21. Sossin WS, Abrams TW (2009) Evolutionary conservation of the signaling proteins upstream of cyclic AMP-dependent kinase and protein kinase C in gastropod mollusks. Brain Behav Evol 74: 191–205.
22. Ferguson SS (2001) Evolving concepts in G protein-coupled receptor endocytosis: the role in receptor desensitization and signaling. Pharmacol Rev 53: 1–24.
23. Gainetdinov RR, Premont RT, Bohn LM, Lefkowitz RJ, Caron MG (2004) Desensitization of G protein-coupled receptors and neuronal functions. Annu Rev Neurosci 27: 107–144.
24. Hanyaloglu AC, von Zastrow M (2008) Regulation of GPCRs by endocytic membrane trafficking and its potential implications. Annu Rev Pharmacol Toxicol 48: 537–568.
25. Farah CA, Nagakura I, Weatherill D, Fan X, Sossin WS (2008) Physiological role for phosphatidic acid in the translocation of the novel protein kinase C Apl II in Aplysia neurons. Mol Cell Biol 28: 4719–4733.
26. Pettigrew DB, Smolen P, Baxter DA, Byrne JH (2005) Dynamic properties of regulatory motifs associated with induction of three temporal domains of memory in aplysia. J Comput Neurosci 18: 163–181.
27. Holmes KD, Babwah AV, Dale LB, Poulter MO, Ferguson SS (2006) Differential regulation of corticotropin releasing factor 1alpha receptor endocytosis and trafficking by beta-arrestins and Rab GTPases. J Neurochem 96: 934–949.
28. Dhami GK, Ferguson SS (2006) Regulation of metabotropic glutamate receptor signaling, desensitization and endocytosis. Pharmacol Ther 111: 260–271.
29. Magalhaes AC, Dunn H, Ferguson SS (2011) Regulation of G Protein-Coupled Receptor Activity, Trafficking and Localization by Gpcr-Interacting Proteins. Br J Pharmacol;doi: 10.1111/j.1476-5381.2011.01552.x.
30. Cao TT, Deacon HW, Reczek D, Bretscher A, von Zastrow M (1999) A kinase-regulated PDZ-domain interaction controls endocytic sorting of the beta2-adrenergic receptor. Nature 401: 286–290.
31. Wang B, Bisello A, Yang Y, Romero GG, Friedman PA (2007) NHERG1 regulates parathyroid hormone receptor membrane retention without affecting recycling. J Biol Chem 282: 36214–36222.
32. Wang B, Bisello A, Yang Y, Romero GG, Friedman PA (2009) NHERF1 regulates parathyroid hormone receptor desensitization: interference with beta-arrestin binding. Mol Pharmacol 75: 1189–1197.
33. Ceci M, Gaviraghi C, Gorrini C, Sala LA, Offenhauser N, et al. (2003) Release of eIF6 (p27BBP) from the 60S subunit allows 80S ribosome assembly. Nature 426: 579–584.
34. Dobrikov M, Dobrikova E, Shveygert M, Gromeier M (2011) Phosphorylation of eukaryotic translation initiation factor 4G1 (eIF4G1) by protein kinase C{alpha} regulates eIF4G1 binding to Mnk1. Mol Cell Biol 31: 2947–2959.
35. Dyer JR, Pepio AM, Yanow SK, Sossin WS (1998) Phosphorylation of eIF4E at a Conserved Serine inAplysia. J Biol Chem 273: 29469.
36. Yanow SK, Manseau F, Hislop J, Castellucci VF, Sossin WS (1998) Biochemical pathways by which serotonin regulates translation in the nervous system of Aplysia. J Neurochem 70: 572–583.
37. Bacskai BJ, Hochner B, Mahaut-Smith M, Adams SR, Kaang BK, et al. (1993) Spatially resolved dynamics of cAMP and protein kinase A subunits in Aplysia sensory neurons. Science 260: 222–226.
38. Bernier L, Castellucci VF, Kandel ER, Schwartz JH (1982) Facilitatory transmitter causes a selective and prolonged increase in adenosine 3′:5′-monophosphate in sensory neurons mediating the gill and siphon withdrawal reflex in Aplysia. J Neurosci 2: 1682–1691.
39. Jean-Alphonse F, Hanyaloglu AC (2010) Regulation of GPCR signal networks via membrane trafficking. Mol Cell Endocrinol 331: 205–214.
40. Lelouvier B, Tamagno G, Kaindl AM, Roland A, Lelievre V, et al. (2008) Dynamics of somatostatin type 2A receptor cargoes in living hippocampal neurons. J Neurosci 28: 4336–4349.
41. Thompson D, Pusch M, Whistler JL (2007) Changes in G protein-coupled receptor sorting protein affinity regulate postendocytic targeting of G protein-coupled receptors. J Biol Chem 282: 29178–29185.
42. Philip F, Sengupta P, Scarlata S (2007) Signaling through a G Protein-coupled receptor and its corresponding G protein follows a stoichiometrically limited model. J Biol Chem 282: 19203–19216.
43. Hao M, Maxfield FR (2000) Characterization of rapid membrane internalization and recycling. J Biol Chem 275: 15279–15286.
44. Mundell SJ, Pula G, McIlhinney RA, Roberts PJ, Kelly E (2004) Desensitization and internalization of metabotropic glutamate receptor 1a following activation of heterologous Gq/11-coupled receptors. Biochemistry 43: 7541–7551.
45. Romero G, von Zastrow M, Friedman PA (2011) Role of PDZ Proteins in Regulating Trafficking, Signaling, and Function of GPCRs Means, Motif, and Opportunity. Adv Pharmacol 62: 279–314.
46. Colledge M, Snyder EM, Crozier RA, Soderling JA, Jin Y, et al. (2003) Ubiquitination regulates PSD-95 degradation and AMPA receptor surface expression. Neuron 40: 595–607.
47. Lee CC, Huang CC, Wu MY, Hsu KS (2005) Insulin stimulates postsynaptic density-95 protein translation via the phosphoinositide 3-kinase-Akt-mammalian target of rapamycin signaling pathway. J Biol Chem 280: 18543–18550.
48. Erdmann KS, Kuhlmann J, Lessmann V, Herrmann L, Eulenburg V, et al. (2000) The Adenomatous Polyposis Coli-protein (APC) interacts with the protein tyrosine phosphatase PTP-BL via an alternatively spliced PDZ domain. Oncogene 19: 3894–3901.
49. Hu Y, Barzilai A, Chen M, Bailey CH, Kandel ER (1993) 5-HT and cAMP induce the formation of coated pits and vesicles and increase the expression of clathrin light chain in sensory neurons of aplysia. Neuron 10: 921–929.
50. Boulant S, Kural C, Zeeh JC, Ubelmann F, Kirchhausen T (2011) Actin dynamics counteract membrane tension during clathrin-mediated endocytosis. Nat Cell Biol 13: 1124–1131.

51. Poupon V, Girard M, Legendre-Guillemin V, Thomas S, Bourbonniere L, et al. (2008) Clathrin light chains function in mannose phosphate receptor trafficking via regulation of actin assembly. Proc Natl Acad Sci U S A 105: 168–173.
52. Park S, Park JM, Kim S, Kim JA, Shepherd JD, et al. (2008) Elongation factor 2 and fragile X mental retardation protein control the dynamic translation of Arc/Arg3.1 essential for mGluR-LTD. Neuron 59: 70–83.
53. Villareal G, Li Q, Cai D, Glanzman DL (2007) The role of rapid, local, postsynaptic protein synthesis in learning-related synaptic facilitation in aplysia. Curr Biol 17: 2073–2080.
54. Antonov I, Kandel ER, Hawkins RD (2010) Presynaptic and postsynaptic mechanisms of synaptic plasticity and metaplasticity during intermediate-term memory formation in Aplysia. J Neurosci 30: 5781–5791.
55. Rao VR, Pintchovski SA, Chin J, Peebles CL, Mitra S, et al. (2006) AMPA receptors regulate transcription of the plasticity-related immediate-early gene Arc. Nat Neurosci 9: 887–895.
56. Messaoudi E, Kanhema T, Soule J, Tiron A, Dagyte G, et al. (2007) Sustained Arc/Arg3.1 synthesis controls long-term potentiation consolidation through regulation of local actin polymerization in the dentate gyrus in vivo. J Neurosci 27: 10445–10455.
57. Likhoshvai V, Ratushny A (2007) Generalized hill function method for modeling molecular processes. J Bioinform Comput Biol 5: 521–531.
58. Woo NH, Duffy SN, Abel T, Nguyen PV (2003) Temporal spacing of synaptic stimulation critically modulates the dependence of LTP on cyclic AMP-dependent protein kinase. Hippocampus 13: 293–300.
59. Scharf MT, Woo NH, Lattal KM, Young JZ, Nguyen PV, et al. (2002) Protein synthesis is required for the enhancement of long-term potentiation and long-term memory by spaced training. J Neurophysiol 87: 2770–2777.
60. Kim M, Huang T, Abel T, Blackwell KT (2010) Temporal sensitivity of protein kinase a activation in late-phase long term potentiation. PLoS Comput Biol 6: e1000691.
61. De Koninck P, Schulman H (1998) Sensitivity of CaM kinase II to the frequency of Ca2+ oscillations. Science 279: 227–230.
62. Genoux D, Haditsch U, Knobloch M, Michalon A, Storm D, et al. (2002) Protein phosphatase 1 is a molecular constraint on learning and memory. Nature 418: 970–975.
63. Yin JC, Del Vecchio M, Zhou H, Tully T (1995) CREB as a memory modulator: induced expression of a dCREB2 activator isoform enhances long-term memory in Drosophila. Cell 81: 107–115.
64. Pagani MR, Oishi K, Gelb BD, Zhong Y (2009) The phosphatase SHP2 regulates the spacing effect for long-term memory induction. Cell 139: 186–198.
65. Philips GT, Tzvetkova EI, Carew TJ (2007) Transient mitogen-activated protein kinase activation is confined to a narrow temporal window required for the induction of two-trial long-term memory in Aplysia. J Neurosci 27: 13701–13705.
66. Costa-Mattioli M, Gobert D, Stern E, Gamache K, Colina R, et al. (2007) eIF2alpha phosphorylation bidirectionally regulates the switch from short- to long-term synaptic plasticity and memory. Cell 129: 195–206.
67. Dong C, Upadhya SC, Ding L, Smith TK, Hegde AN (2008) Proteasome inhibition enhances the induction and impairs the maintenance of late-phase long-term potentiation. Learn Mem 15: 335–347.
68. LeVeque RJ (2007) Finite Difference Methods for Ordinary and Partial Differential Equations. Philadelphia: Society for Industrial and Applied Mathematics.
69. Manseau F, Fan X, Hueftlein T, Sossin W, Castellucci V (2001) Ca2+-independent protein kinase C Apl II mediates the serotonin-induced facilitation at depressed Aplysia sensorimotor synapses. J Neurosci 21: 1247.
70. Pettigrew D, Smolen P, Baxter D, Byrne J (2005) Dynamic properties of regulatory motifs associated with induction of three temporal domains of memory in Aplysia. J Comput Neurosci 18: 163–181.